Investigating the formation, evolution, and properties of high-latitude irregularities and their relevance to magnetosphere-ionosphere-thermosphere coupling

L. V. Goodwin

Email: lindsay.v.goodwin@njit.edu

Early Career Science Highlight - CEDAR 2021

Goodwin, L. V., Iserhienrhien, B., Miles, D. M., Patra, S., van der Meeren, C., Buchert, S. C., Burchill, J.K., Clausen, L. B. N., Knudsen, D. J., McWilliams, K. A., & Moen, J. (2015). Swarm in situ observations of F region polar cap patches created by cusp precipitation. *Geophysical Research Letters*, *42*(4), 996-1003.

Goodwin, L. V., Nishimura, Y., Zou, Y., Shiokawa, K., & Jayachandran, P. T. (2019). Mesoscale Convection Structures Associated With Airglow Patches Characterized Using Cluster-Imager Conjunctions. *Journal of Geophysical Research: Space Physics*, *124*(9), 7513-7532.

Investigating high-latitude irregularities in MIT coupling

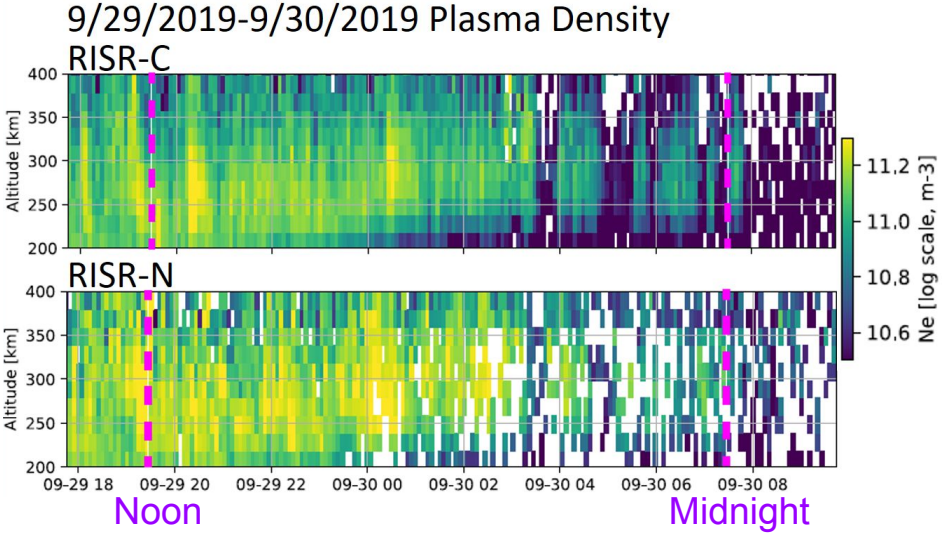

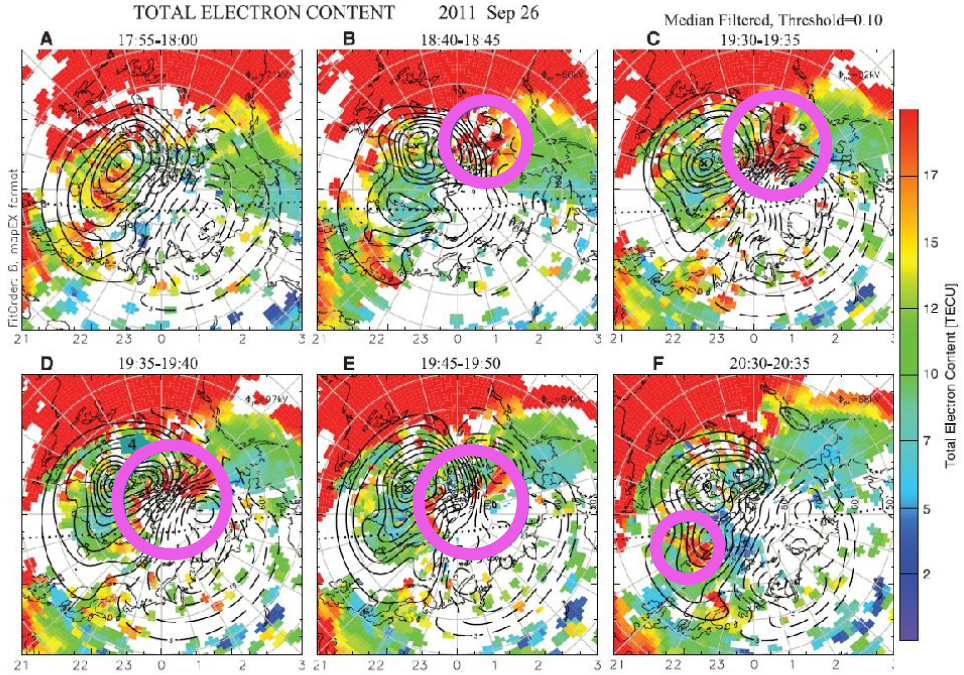

Zhang et al., [2013]

The high-latitude ionosphere is full of “irregularities” (plasma density variations) that evolve in shape and properties as they move along the streamlines of convection.

9/29/2019-9/30/2019 Plasma Density

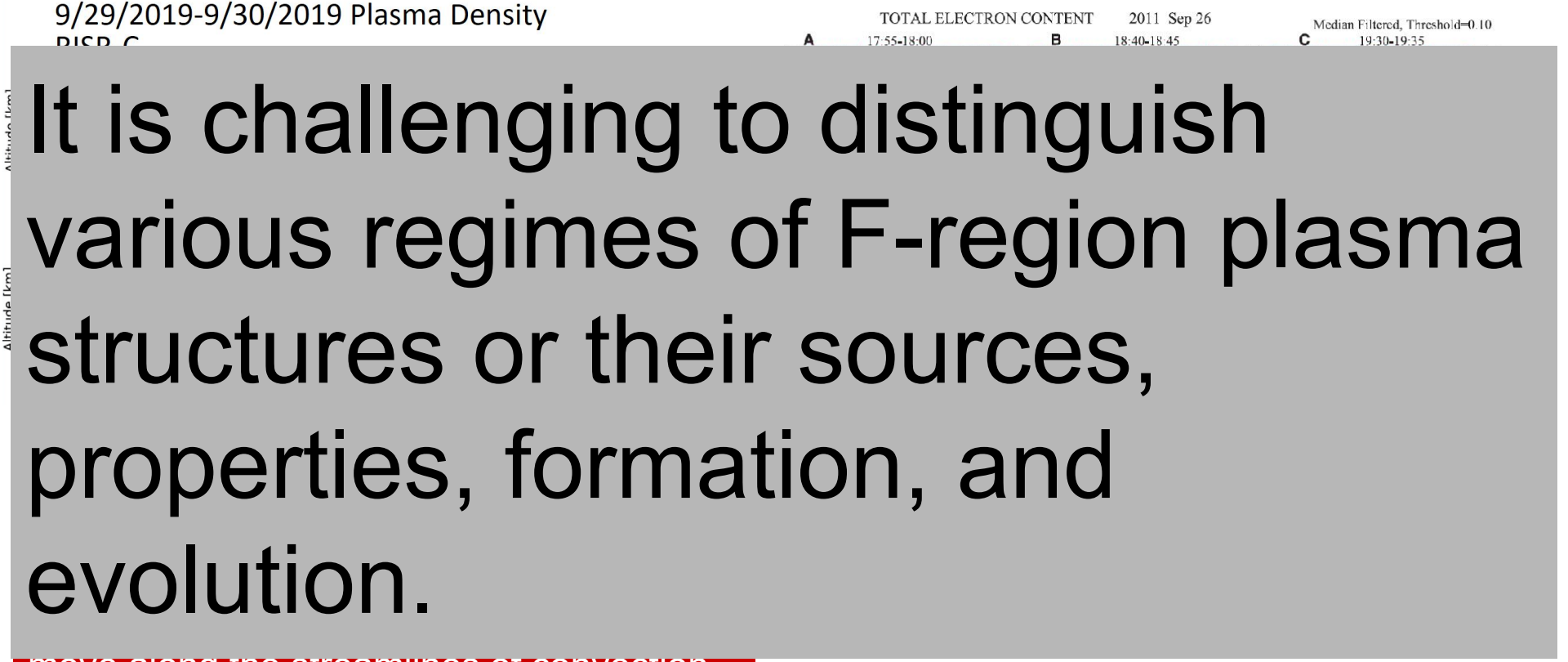

It is challenging to distinguish various regimes of F-region plasma structures or their sources, properties, formation, and evolution.

move along the streamlines of convection.

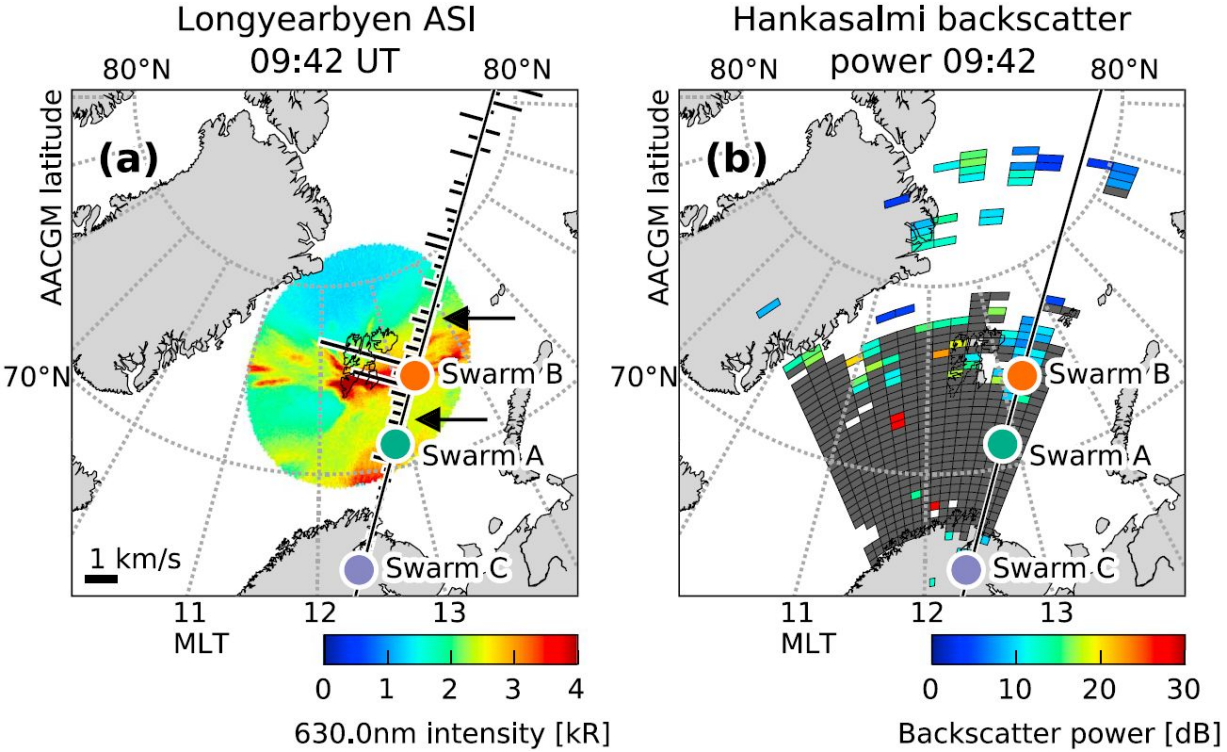

30 December 2013 6-10 Universal Time was a quiet period (Kp = 0-1), where the interplanetary magnetic field was consistently southward and duskward (Bz ≈ -5 nT, By ≈ +2 nT).

Auroral emissions in Svalbard All-Sky Imager data are collocated with SuperDARN backscatter (near cusp) and Swarm B measurements of a relative westward ion flow.

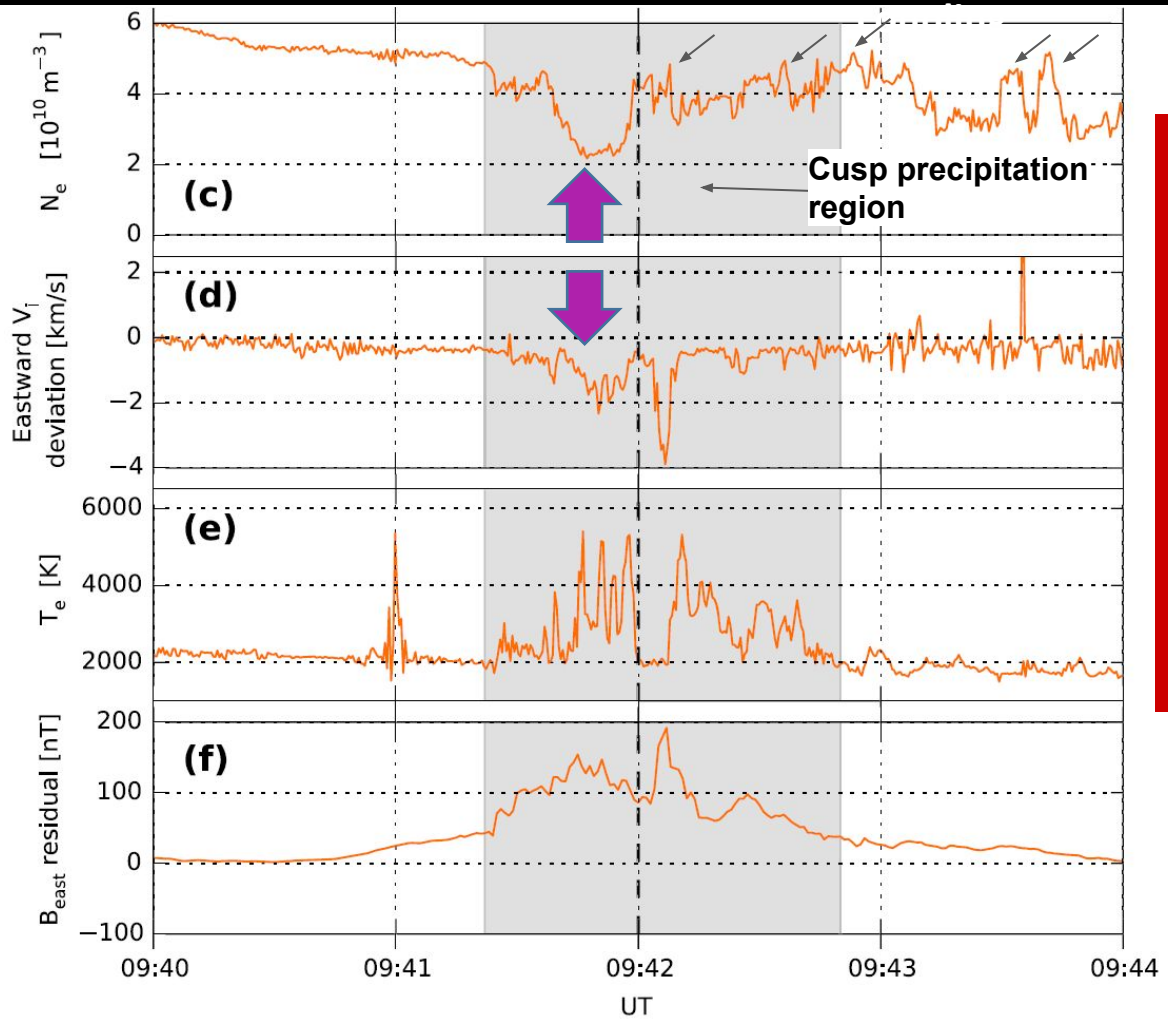

A low-density relatively westward flow channel is transporting plasma from the postnoon sector.

This is consistent with Lockwood et al., [2005] and Zhang et al., [2011] during By>0 conditions.

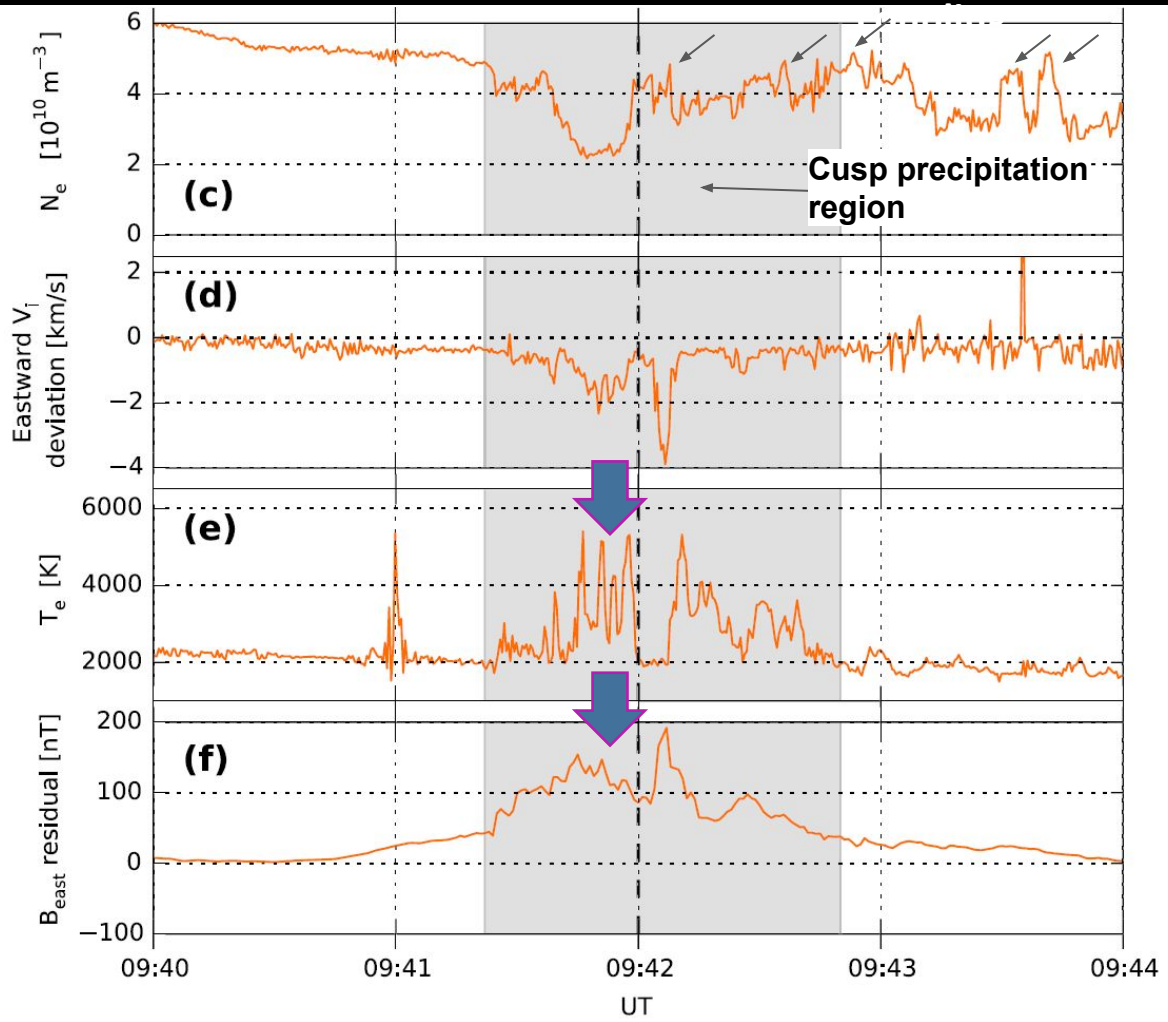

The observed discrete electron temperature enhancements and region of upward FAC in the cusp are consistent with particle impact ionization initializing 10-100 km-scale structures.

This has been similarly seen in Kelley et al., [1982] and Moen et al., [2012].

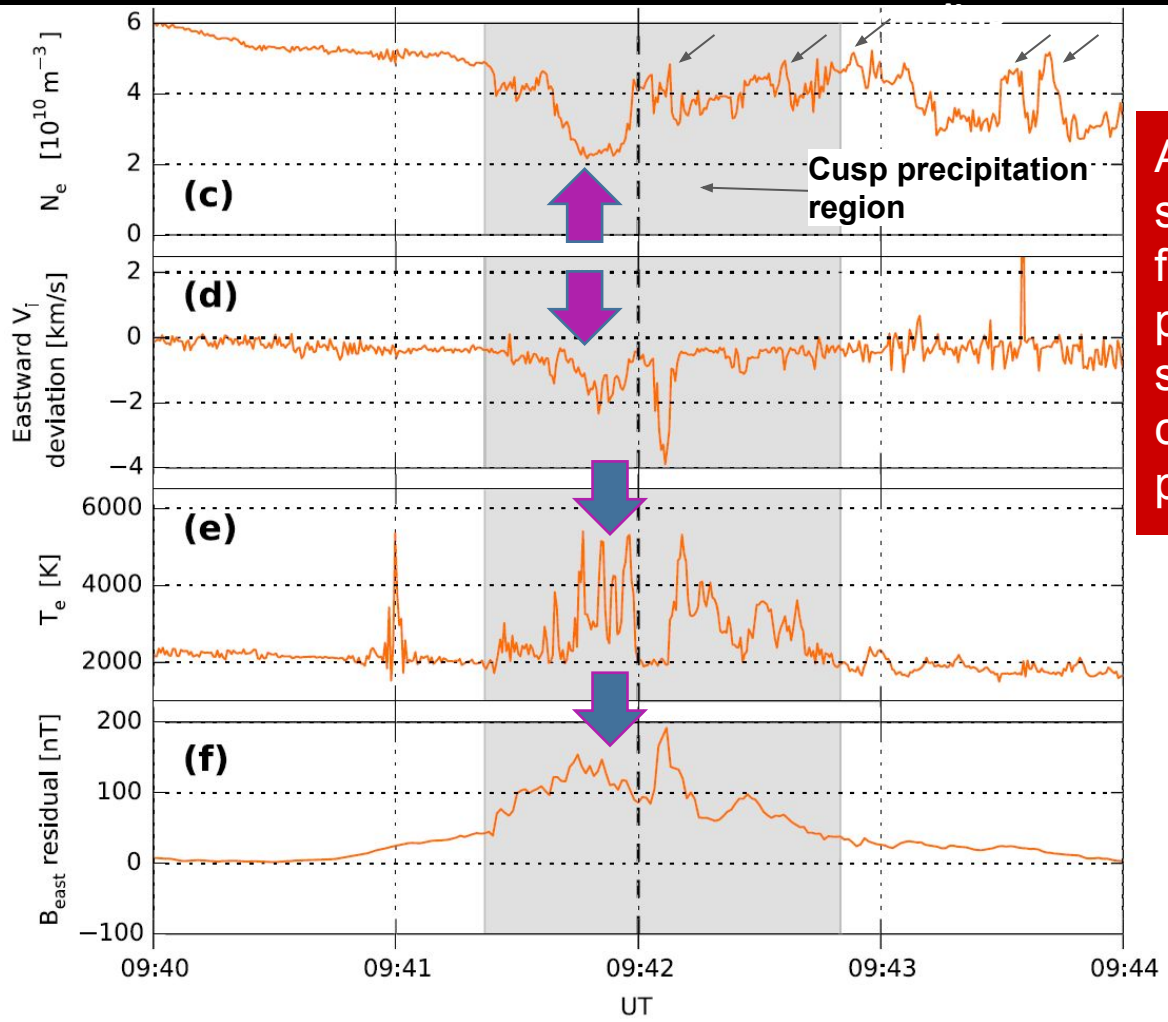

A reconnection driven flow channel separates solar-ionized plasma from a region of active precipitation. Therefore, the structuring poleward of the flow channel must be the result of particle impact ionization.

Sun is 5° below the horizon

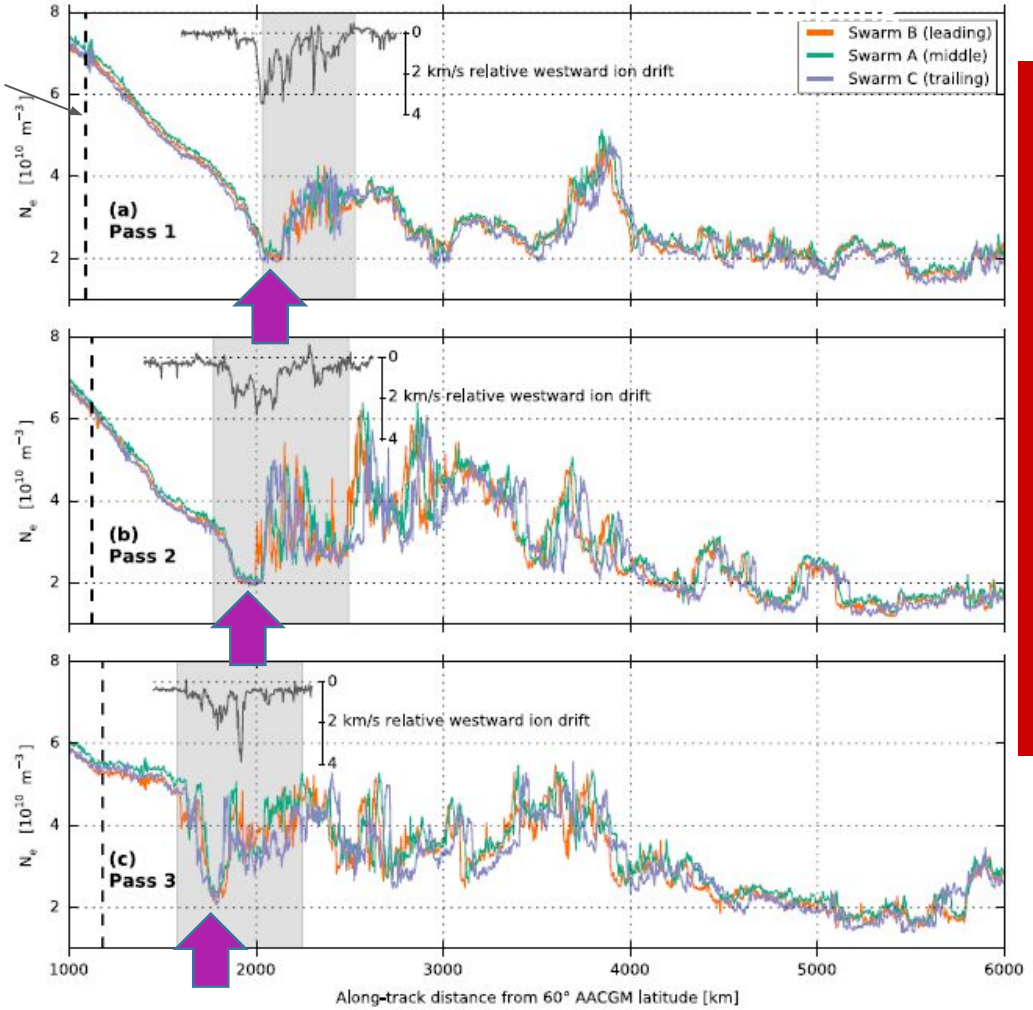

The density depletion and flow channel migrate equatorward, consistent with the expansion of the polar cap during Bz<0.

As the flow channel moves, it erodes and transports solar-ionized plasma, mixing it with low-density plasma from the relative westward flow and incorporating it into the polar cap.

Irregularities become lower density and less structured as they drift along-track.

More mature irregularities show the classic gradient drift instability driven shape (sharp leading edge, relatively flat middle, and a structured-tapered trailing edge), yet the gradient drift instability is not adding structure.

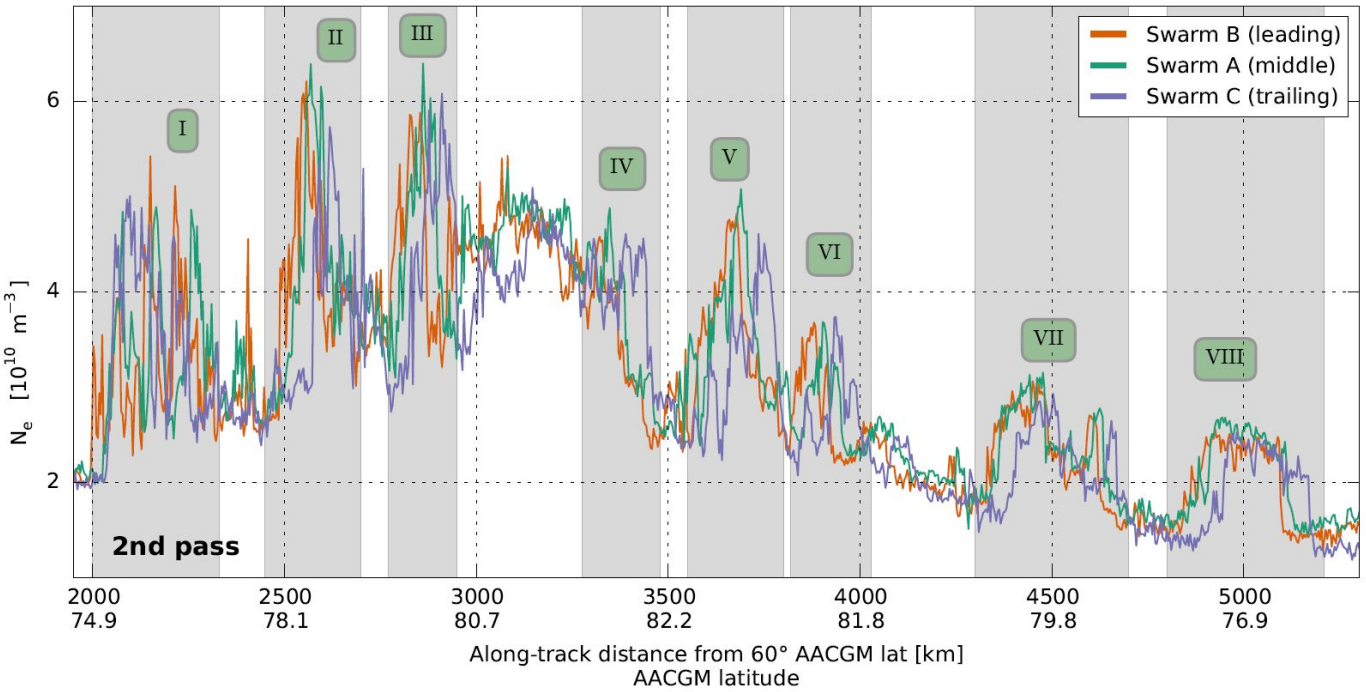

Given that irregularities can be generated through magnetospheric changes (e.g. precipitation and convection), it is worth exploring their magnetospheric signature.

adding structure.

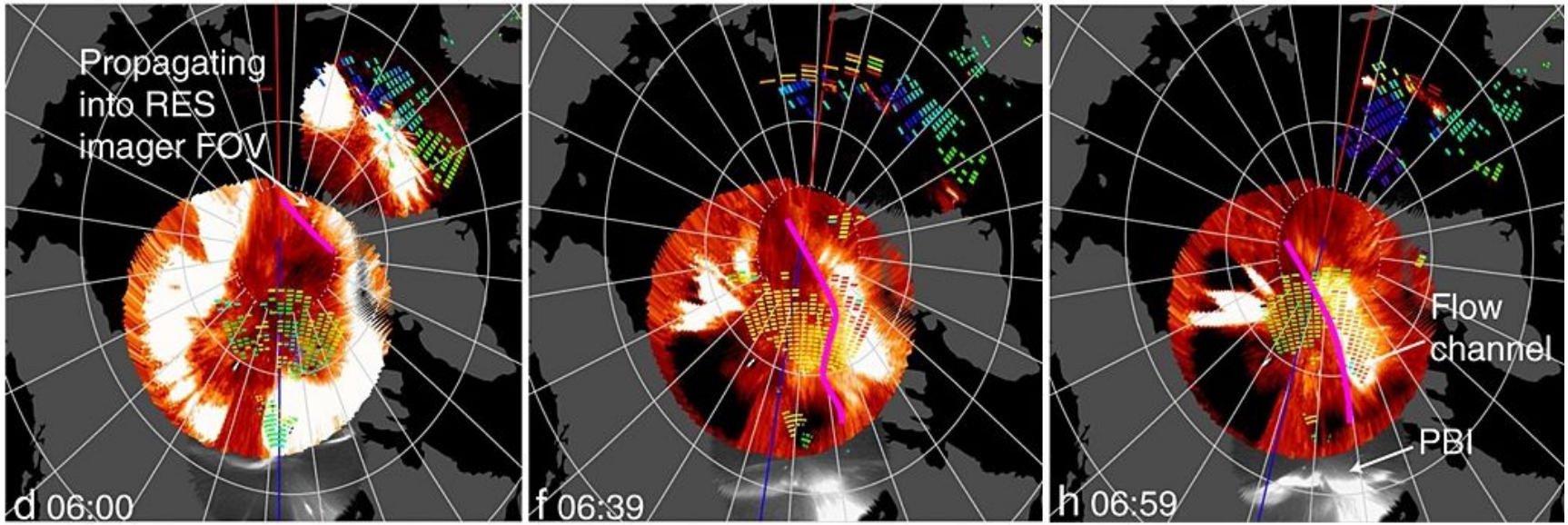

Nishimura et al. [2014]

Irregularities have mesoscale flows embedded within them [Nishimura et al., 2014], and ionospheric mesoscale flows and airglow patches are associated field-aligned currents [Zou et al., 2016] and enhanced localized precipitation [Zou et al., 2017] on open field lines.

However, these and other previous studies can not address the magnetospheric structures driving ionosphere irregularities.

Using the Cluster spacecraft, we examined collocated magnetospheric measurements of red-line airglow enhancements measured from the Resolute Bay Optical Mesosphere Thermosphere Imager.

In this example, we have an enhancement moving primarily antisunward, but also dawnward and then duskward.

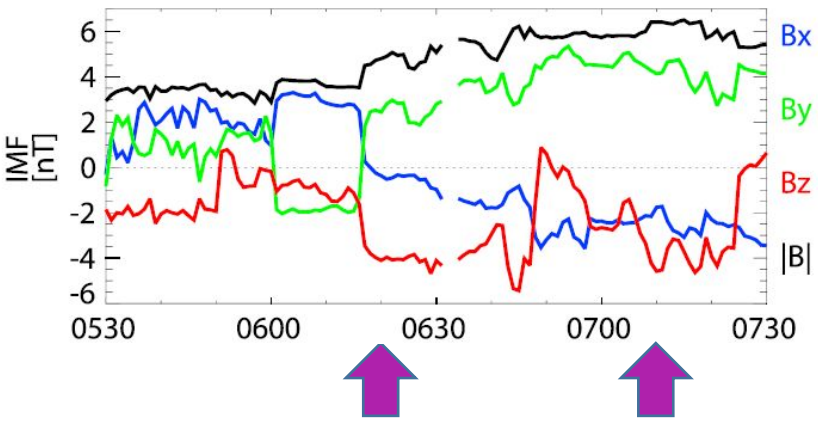

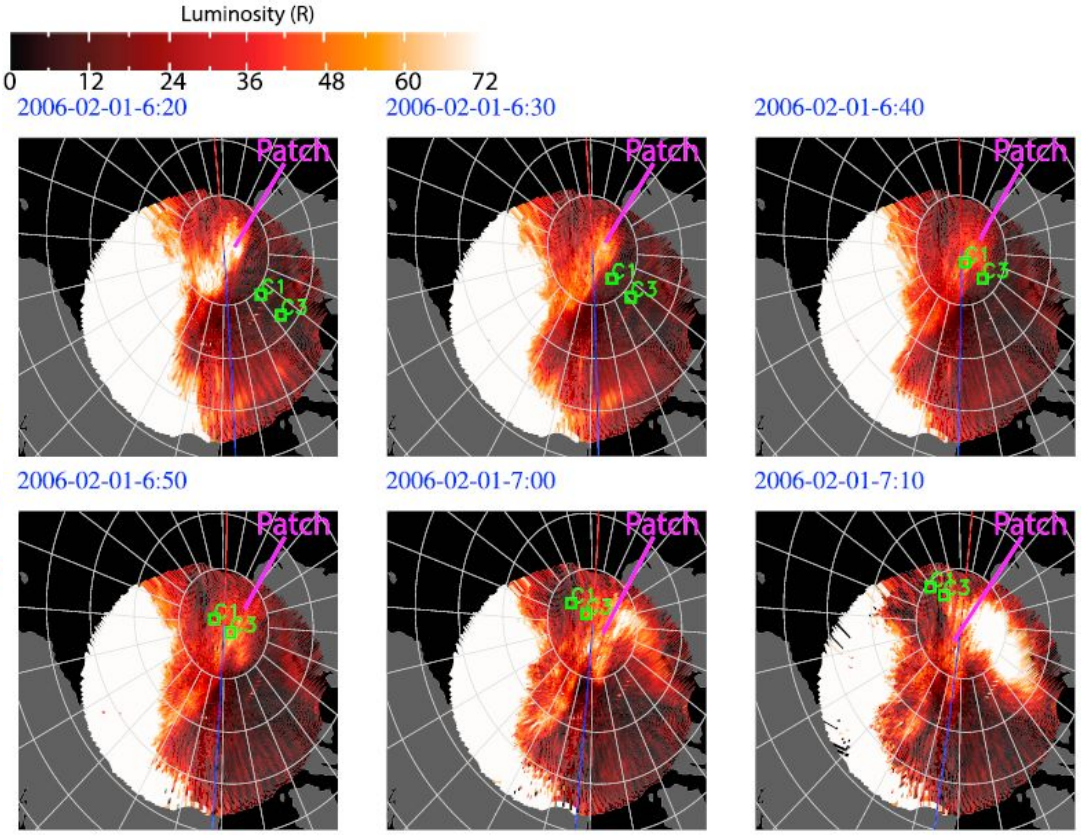

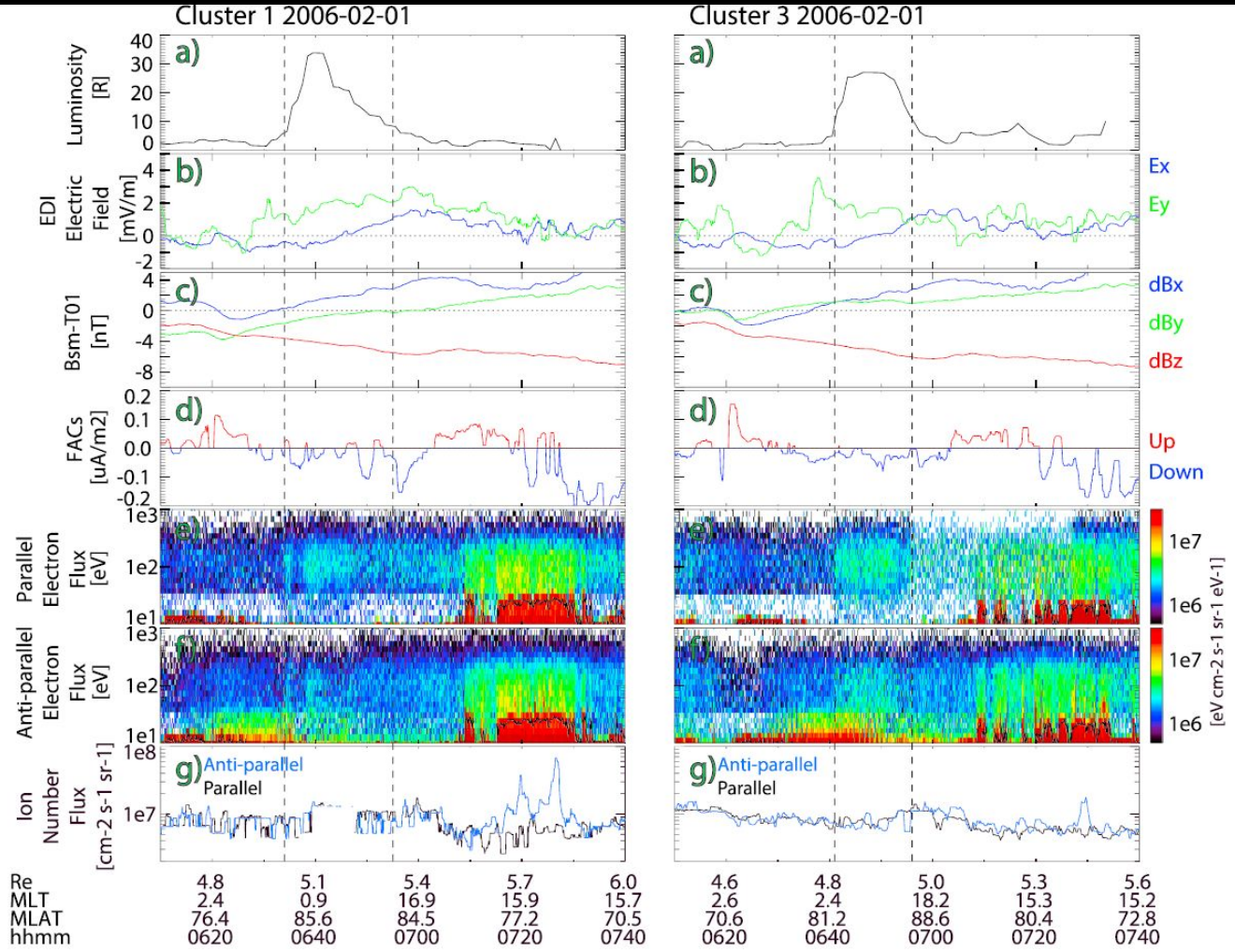

This moving structure shows:

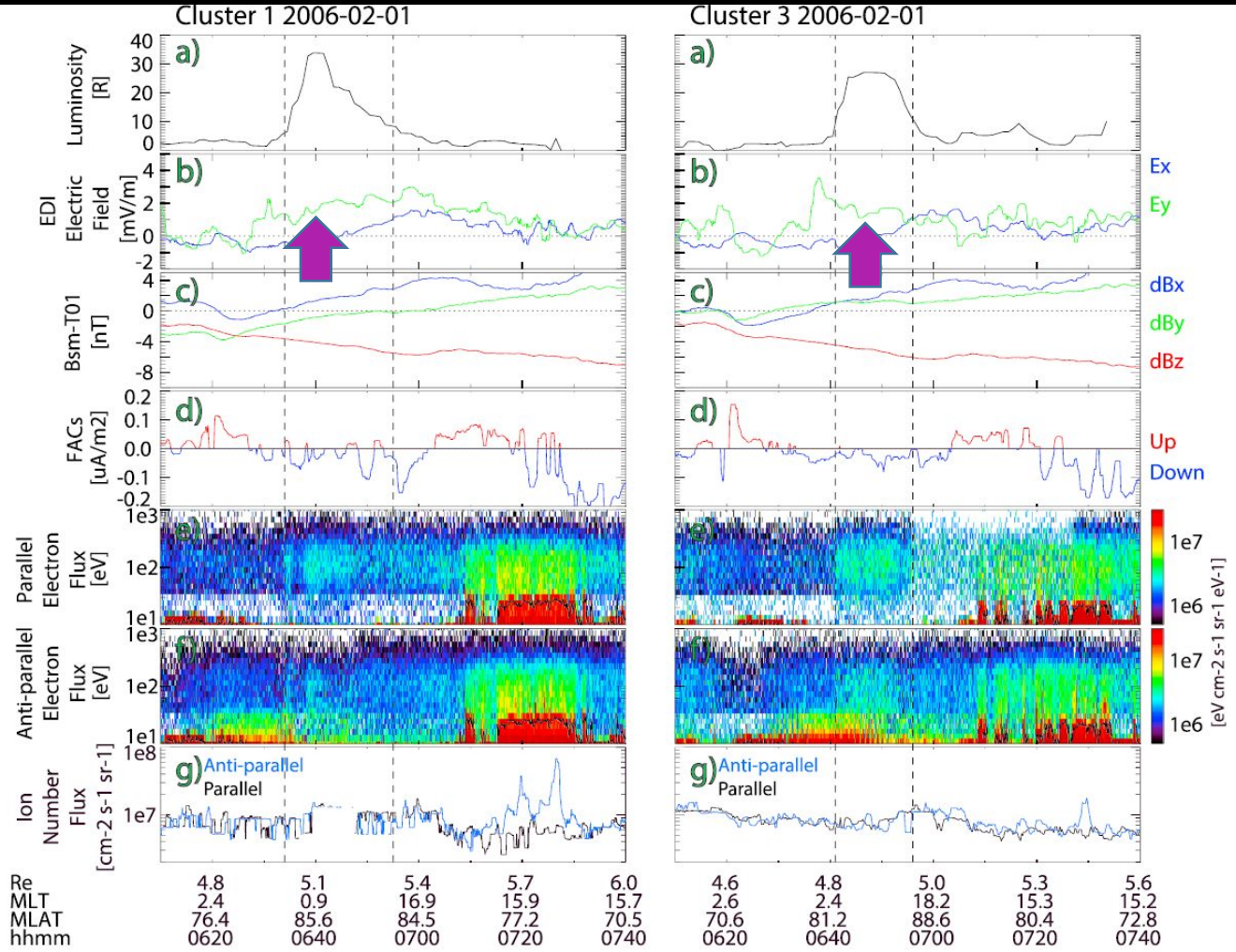

This moving structure shows:

(1) electric field enhancements,

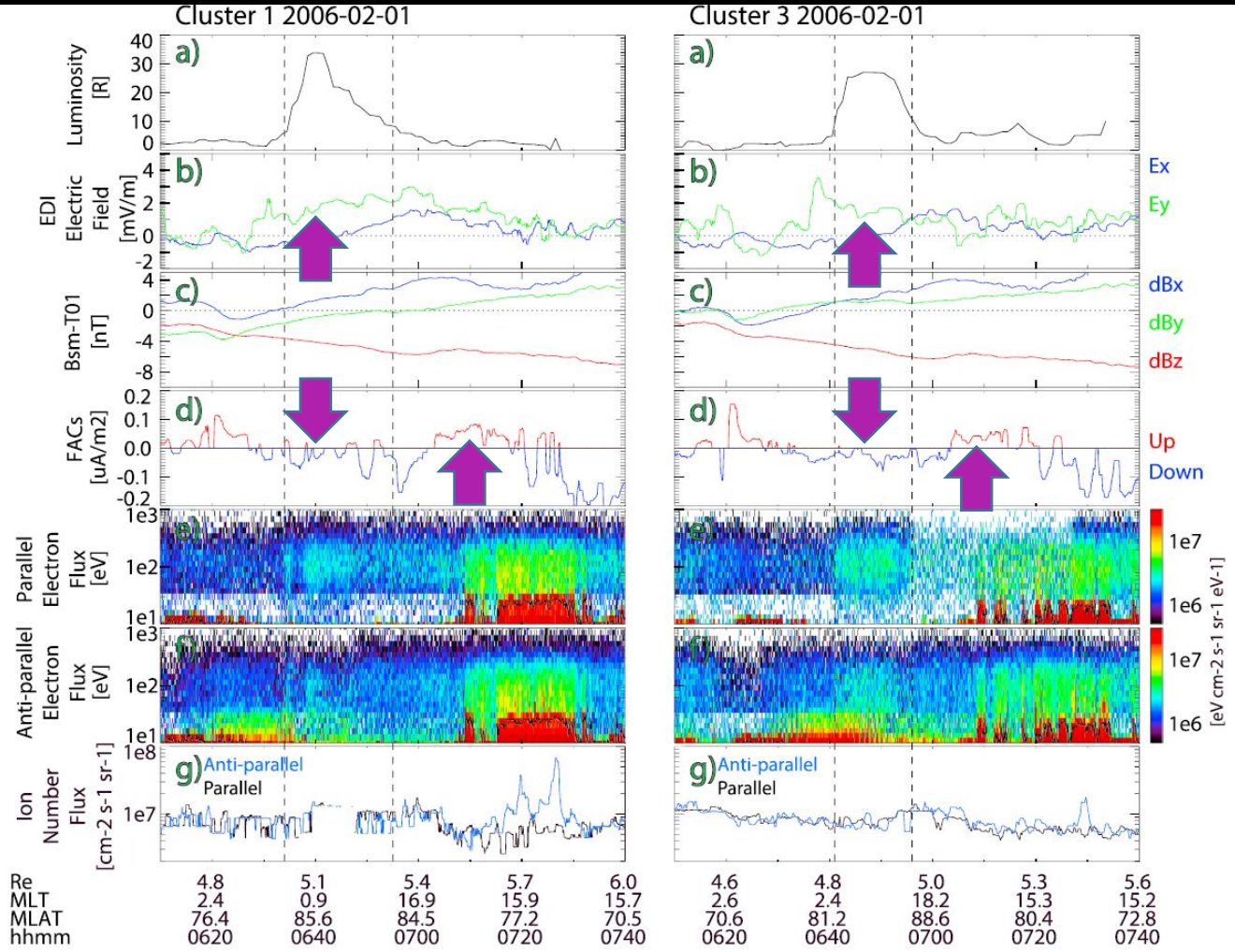

This moving structure shows:

(1) electric field enhancements,

(2) Region 1 sense field-aligned currents,

(3) downward Poynting fluxes,

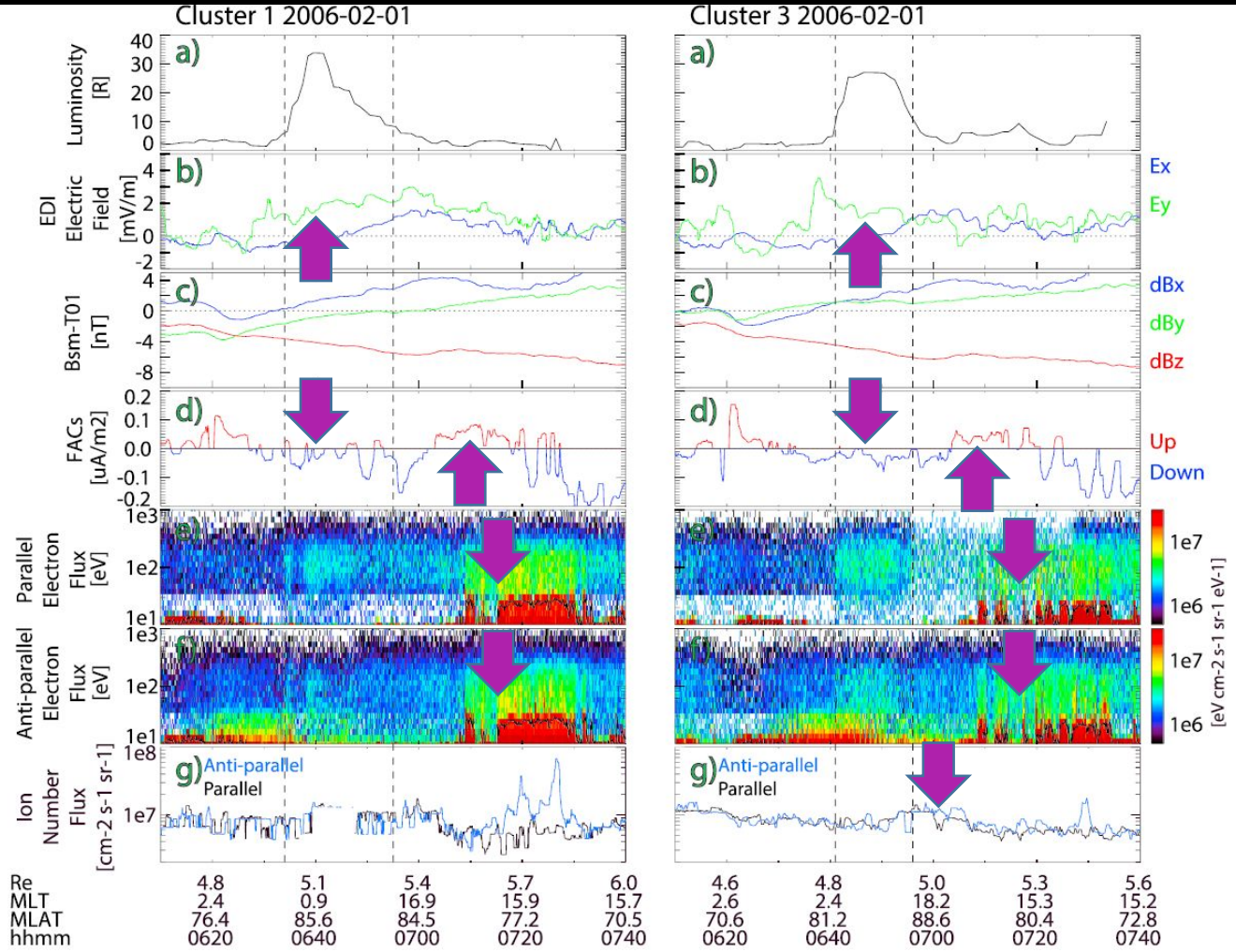

This moving structure shows:

(1) electric field enhancements,

(2) Region 1 sense field-aligned currents,

(3) downward Poynting fluxes,

(4) field-aligned enhancements in soft electron flux and,

(5) enhancements in upward

ion flux (only in some cases)

Investigating high-latitude irregularities in MIT coupling

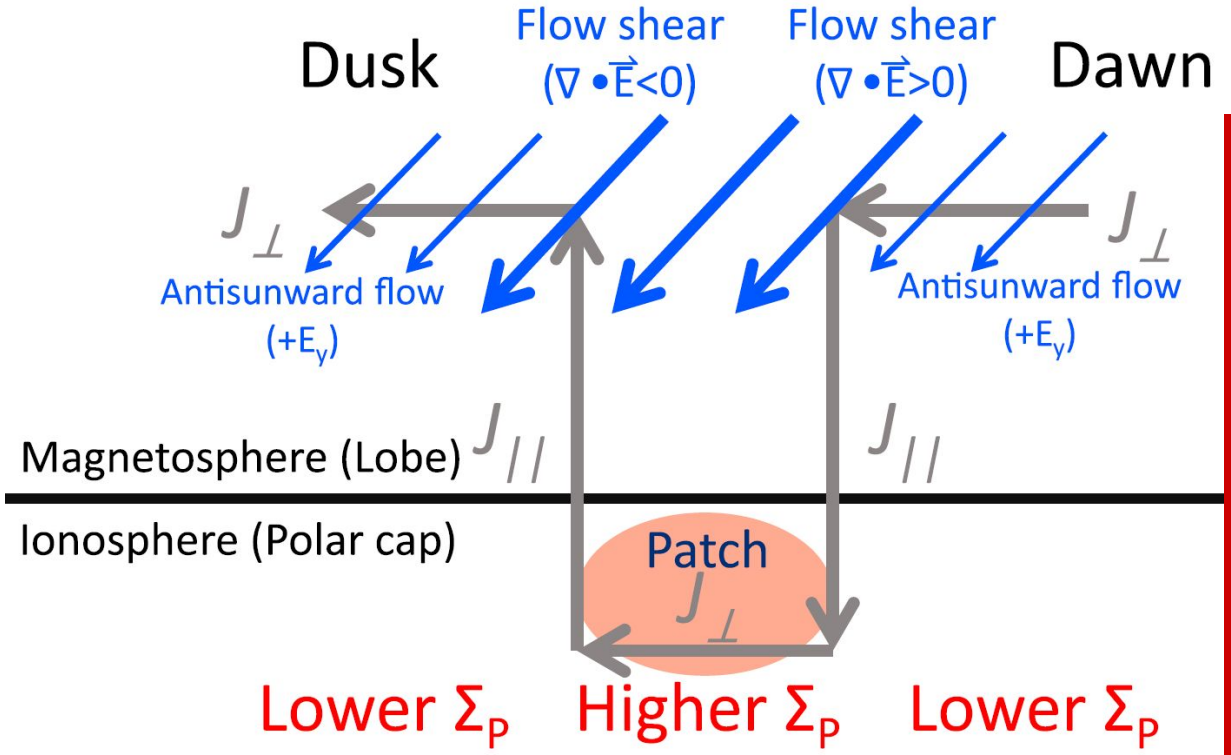

Our observations are consistent with a Pedersen current closing a Region-1 sense FAC pair

Irregularity motion is driven by the localized electric field in the magnetosphere, not the thermosphere.

Irregularities are a signature of enhancements in dayside magnetospheric reconnection and the enhanced propagation of open flux tubes.

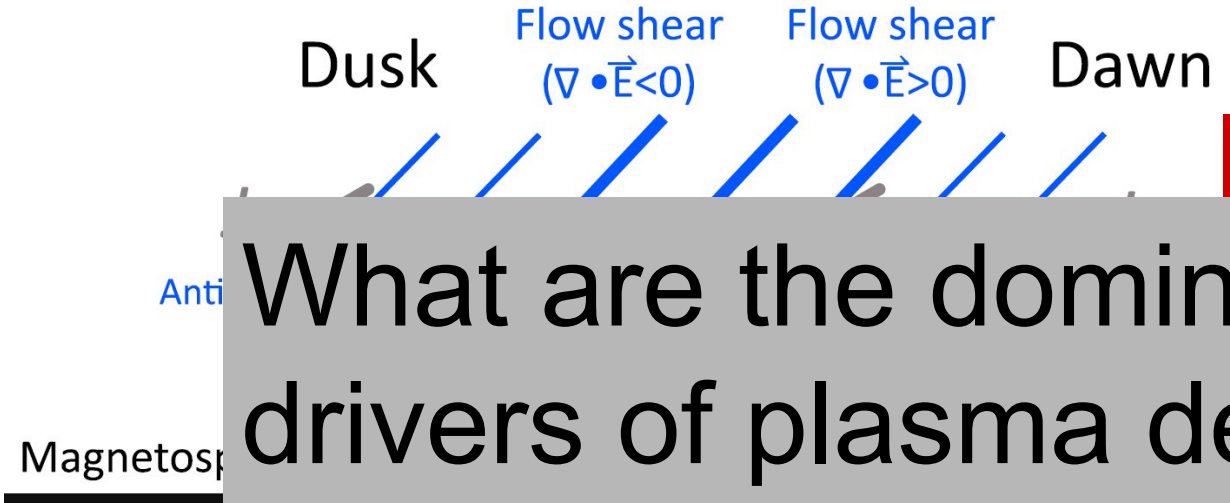

Our observations are
rsen
on-1
riven by
eld in the
e
nature of
ide
nection
pagation

What are the dominant drivers of plasma density irregularities, their different scale-sizes, and their different properties?

Using novel Incoherent Scatter Radar techniques, high-latitude irregularities are resolved at a finer spatio-temporal resolution than has been previously possible with ground-based observations.

Check-out my poster: **ITIT-14**

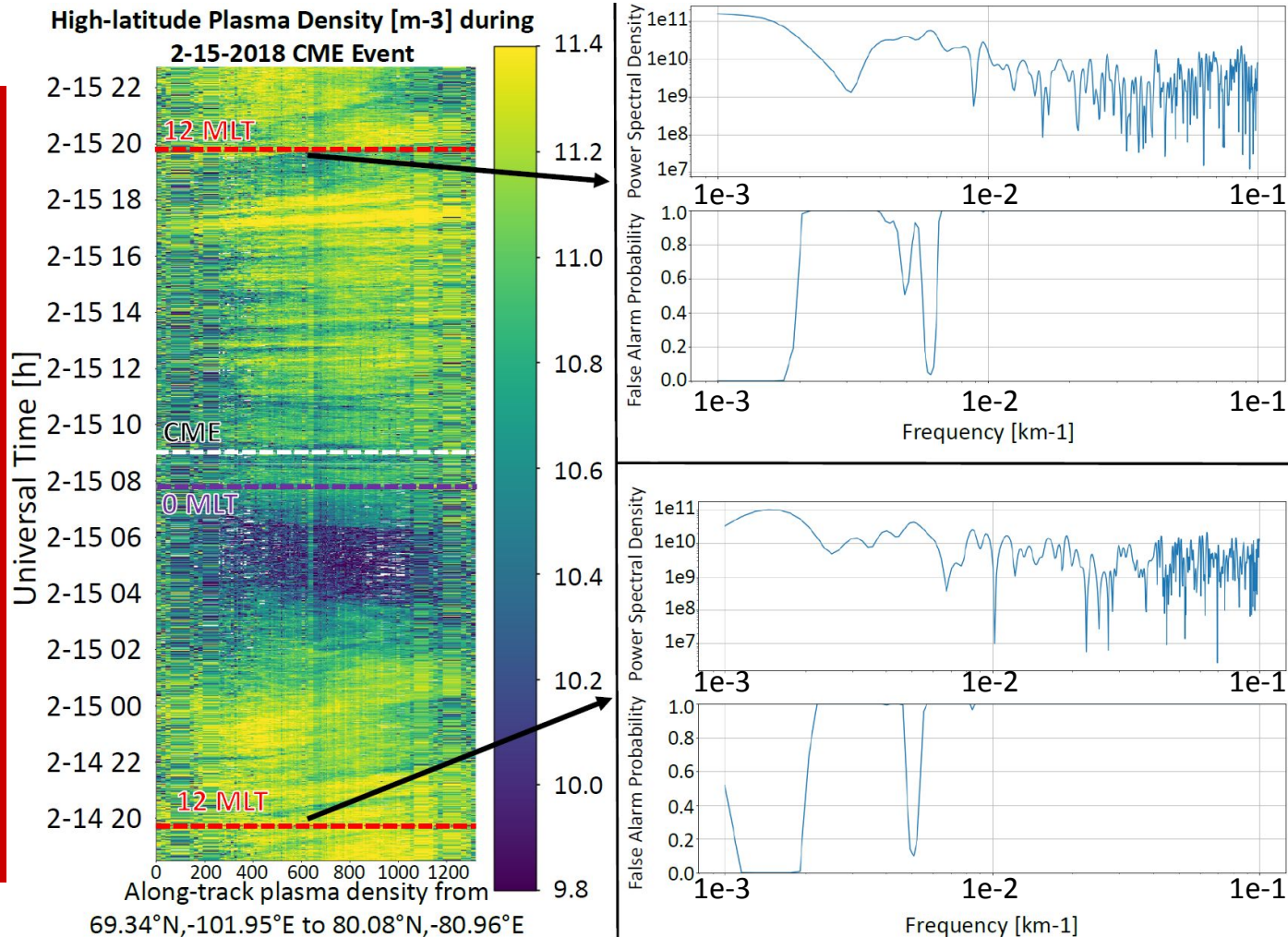

“Swarm in situ observations of F region polar cap patches created by cusp precipitation” [Goodwin, et al., 2015]

- This study shows the first in situ observations tracking plasma irregularity evolution from creation by plasma transport and enhancement by cusp precipitation, through entrainment in the polar cap flow and relaxation into smooth structures as they approach the nightside auroral oval.

“Mesoscale Convection Structures Associated With Airglow Patches Characterized Using Cluster-Imager Conjunctions” [Goodwin, et al., 2019]

- This work explores the magnetospheric counterpart of enhancements and highlights the importance of viewing them as structures driven by the magnetosphere, and not just localized enhancements that exist within the ionosphere.
  - Moving plasma density structures shows: (1) electric field enhancements, (2) Region-1 sense field-aligned currents, (3) downward Poynting fluxes, (4) field-aligned enhancements in soft electron flux and, (5) enhancements in ion flux (only in some cases)

“Using novel geospace sensor techniques to resolve high-latitude ionospheric plasma density structures and their solar drivers” [in preparation]

- Using novel ISR techniques and observational methods, high-latitude irregularities are resolved at a finer spatio-temporal resolution than has been previously possible with ground-based observations.

Thank you for your attention, and to all of my colleagues!

Past and Present supervisors: **J.-P. St.-Maurice, Y. Nishimura, and G. W. Perry**

Co-authors on mentioned publications: B. Iserhienrhien, D. M. Miles, S. Patra, C. van der Meeren, S. C. Buchert, J. K. Burchill, L. B. N. Clausen, D. J. Knudsen, **K. A. McWilliams**, J. Moen, Y. Nishimura, Y. Zou, K. Shiokawa, P. T. Jayachandran, A. J. Coster, S. Zhang, N. Nishitani, J. M. Ruohoniemi, B. J. Anderson, and Q.-H. Zhang

Other important "Shout-outs": The **CEDAR Science Steering Committee**

Canada-Norway Rocket Science Training and Educational Program (CaNoRock STEP): R. Floberghagen, J. Rauberg, C. Stolle, European Space Agency, Norwegian Research Council, Radio and Space Plasma Physics Group at the University of Leicester, the Goddard Space Flight Center/Space Physics Data Facility OMNIWeb interface, Research Council of Norway, Natural Sciences and Engineering Research Council, Canadian Space Agency, and the Norwegian Centre for International Cooperation in Education, Andøya Space Center, University of Alberta, University of Bergen, University of Calgary, University of Oslo, University of Saskatchewan, University of Tromsø, and the University Centre in Svalbard.

National Aeronautics and Space Administration and National Science Foundation, Japan Society for the Promotion of Science, K. Hosokawa, and the Cluster spacecraft team.

SRI International, SuperMAG, and **NASA Living With a Star Jack Eddy Postdoctoral Fellowship Program**, administered by UCAR's Cooperative Programs for the Advancement of Earth System Science (CPAESS).

Back-up Slides

Epoch study with respect to the dawnward edge of each patch.

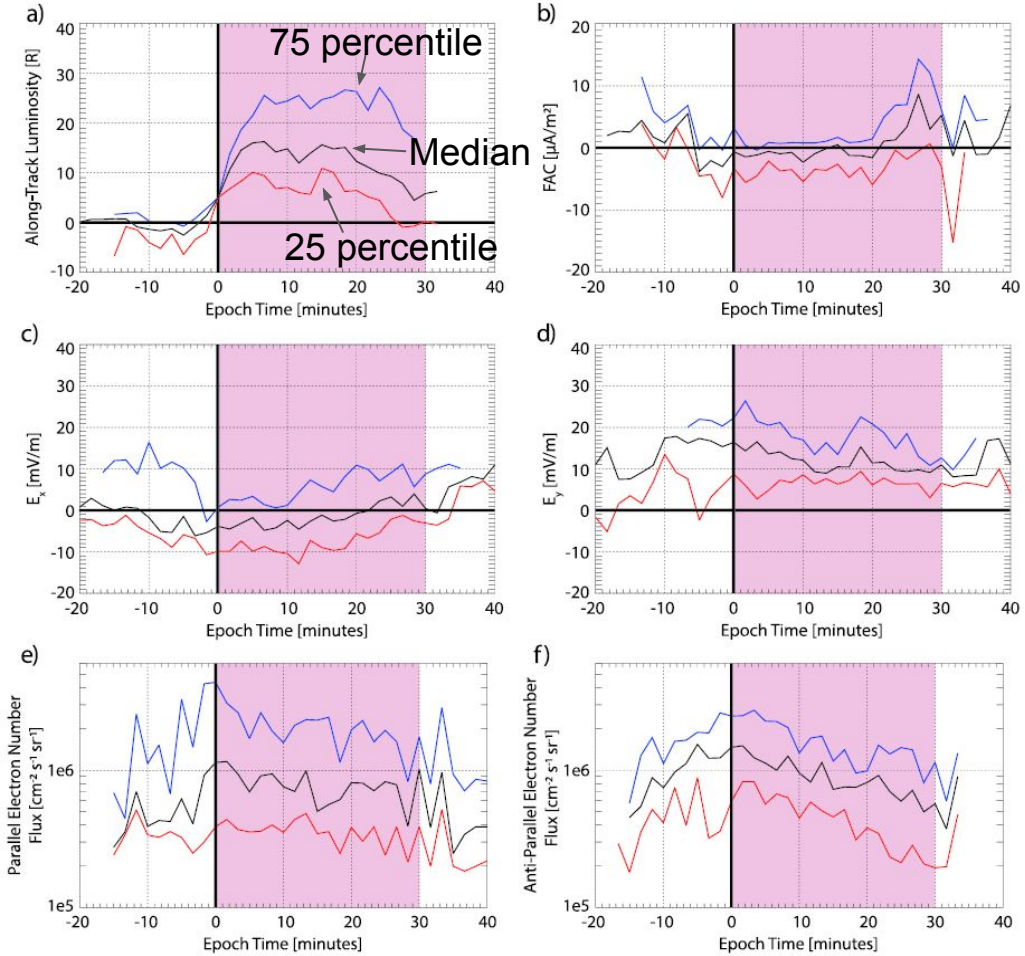

38 events conjugate events from 2005 to 2009 are identified and used to determine the “typical” magnetospheric signature of an enhancement.

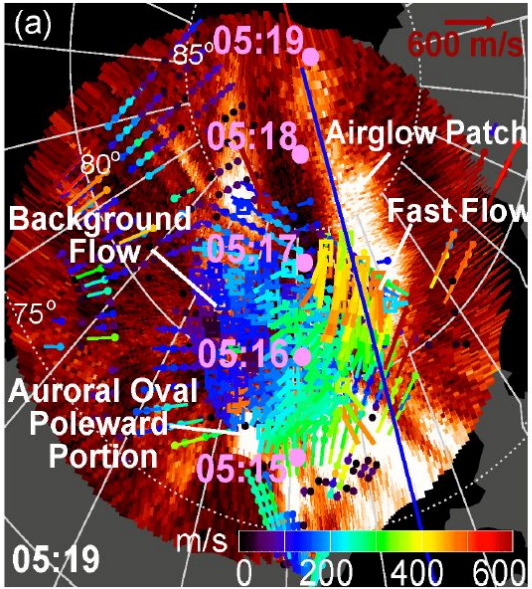

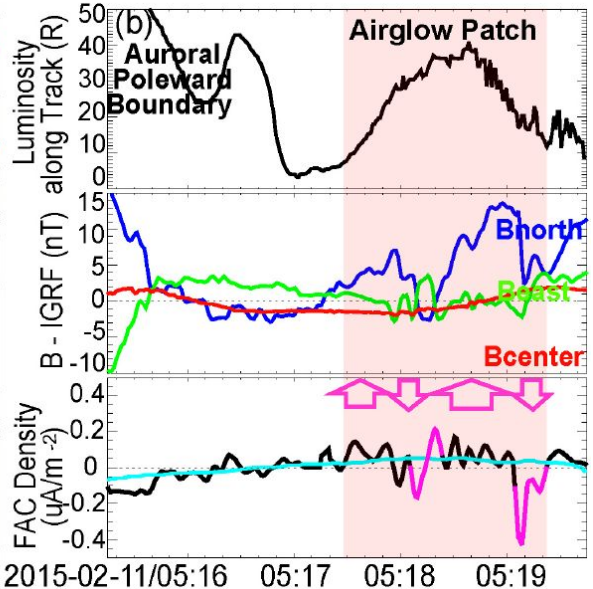

Zou et al. [2016].

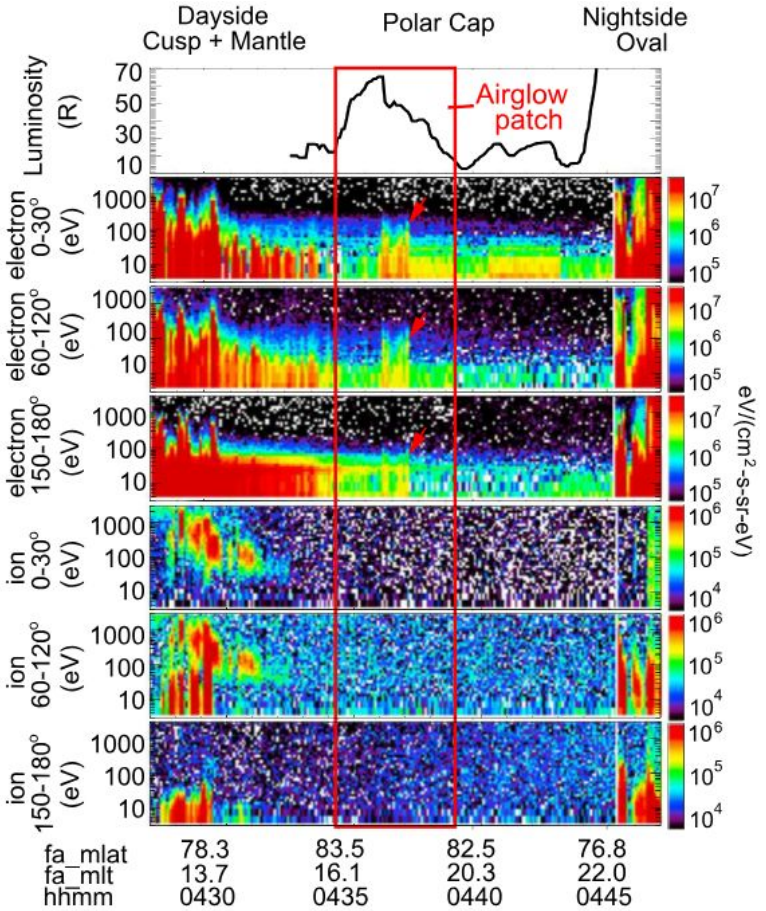

Zou et al. (2017).

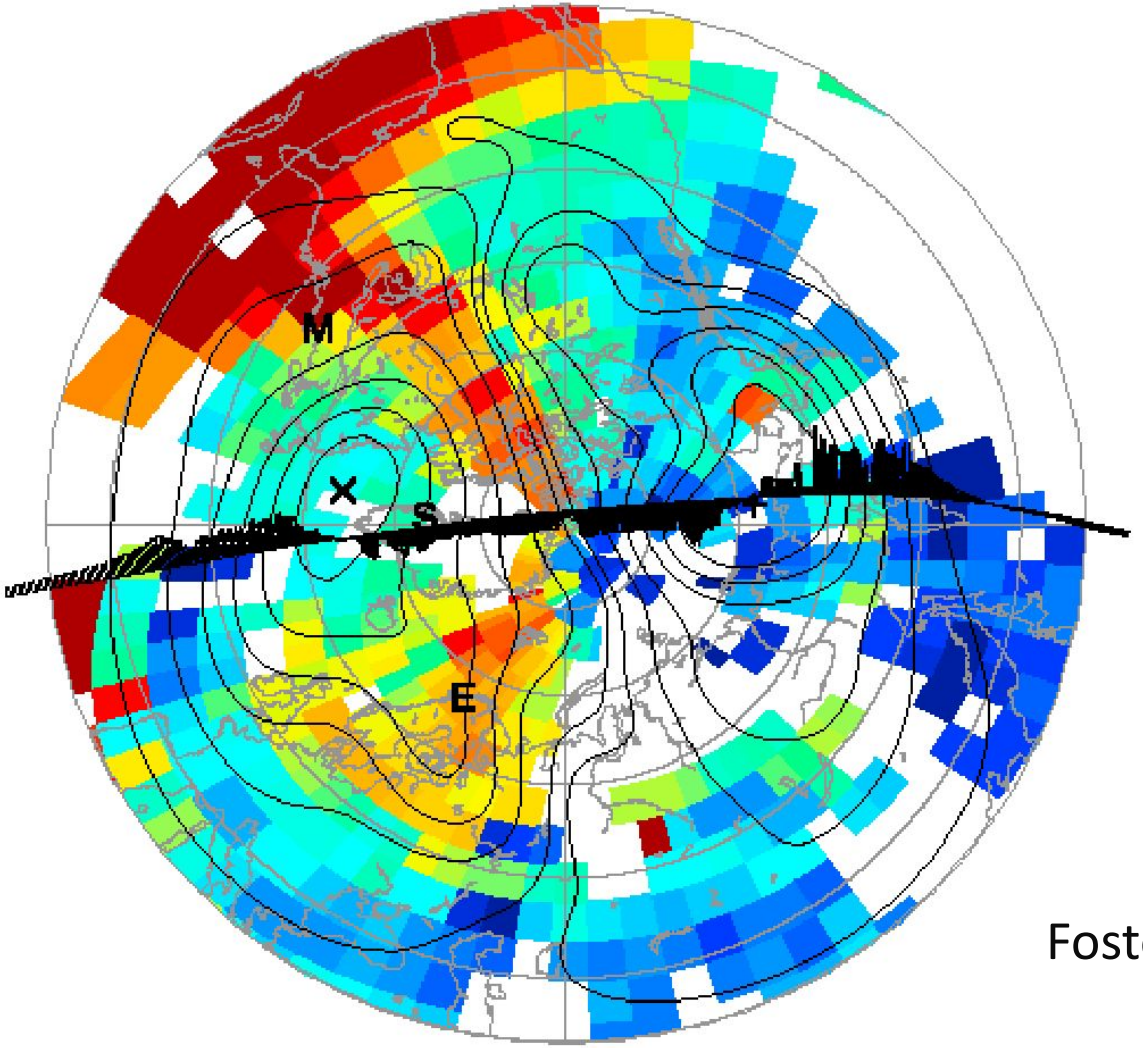

Emerging from an plasma density plume at lower latitudes during a geomagnetic storm, a high-density plasma structure moves into and across the polar cap along plasma convection streams.

Foster et al., [2005]

Plasma transport can generate islands of plasma enhancements and depletions in the high-latitude ionosphere.

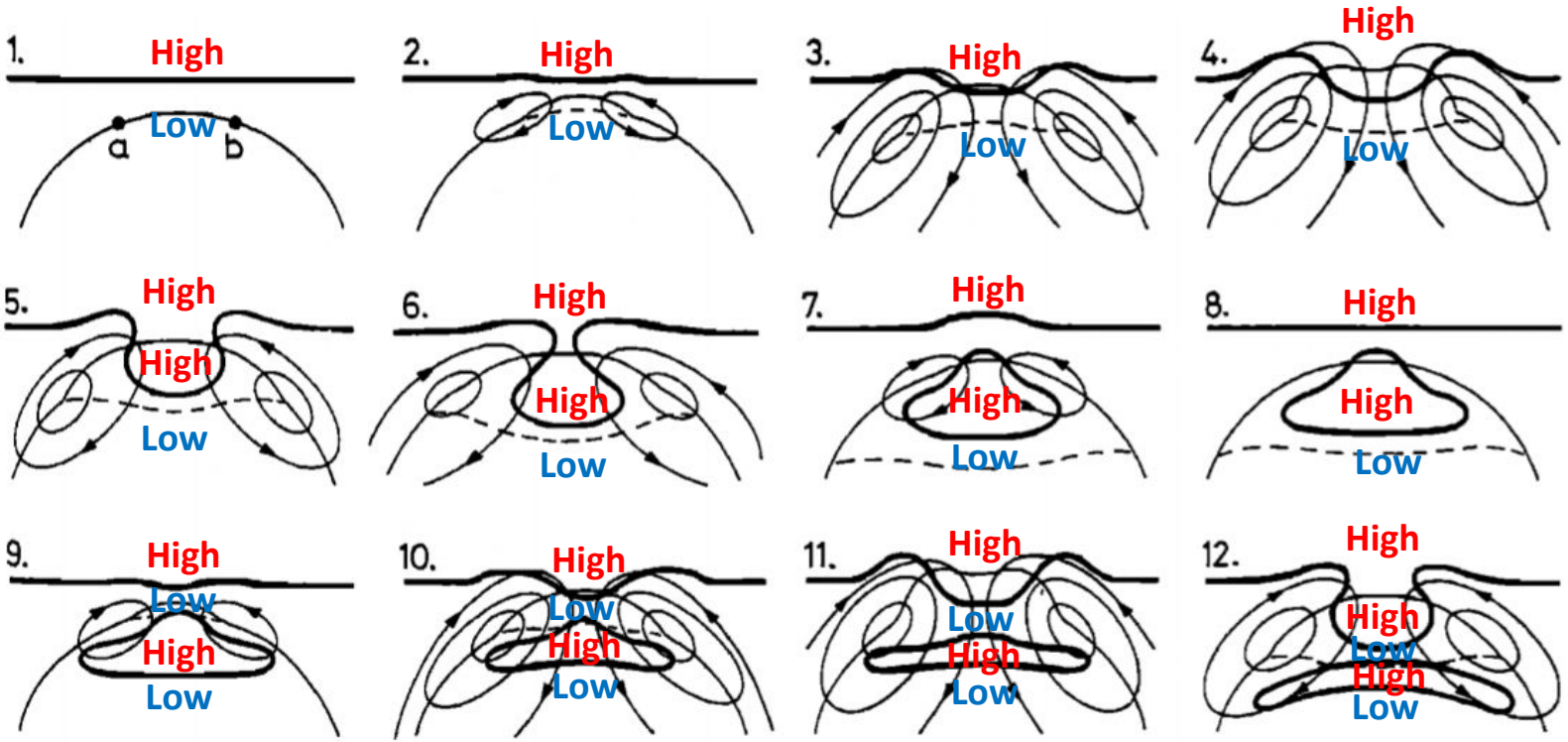

Lockwood and Carlson Jr, [1992]

Case 2

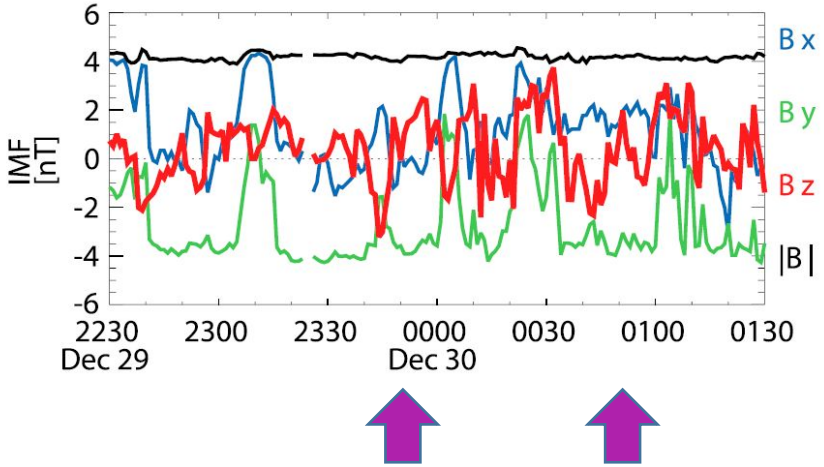
IMF [nT]
6
4
2
0
-2
-4
-6
2230
2300
2330
0000
0030
0100
0130
Dec 29
Dec 30
B x
B y
B z
|B|

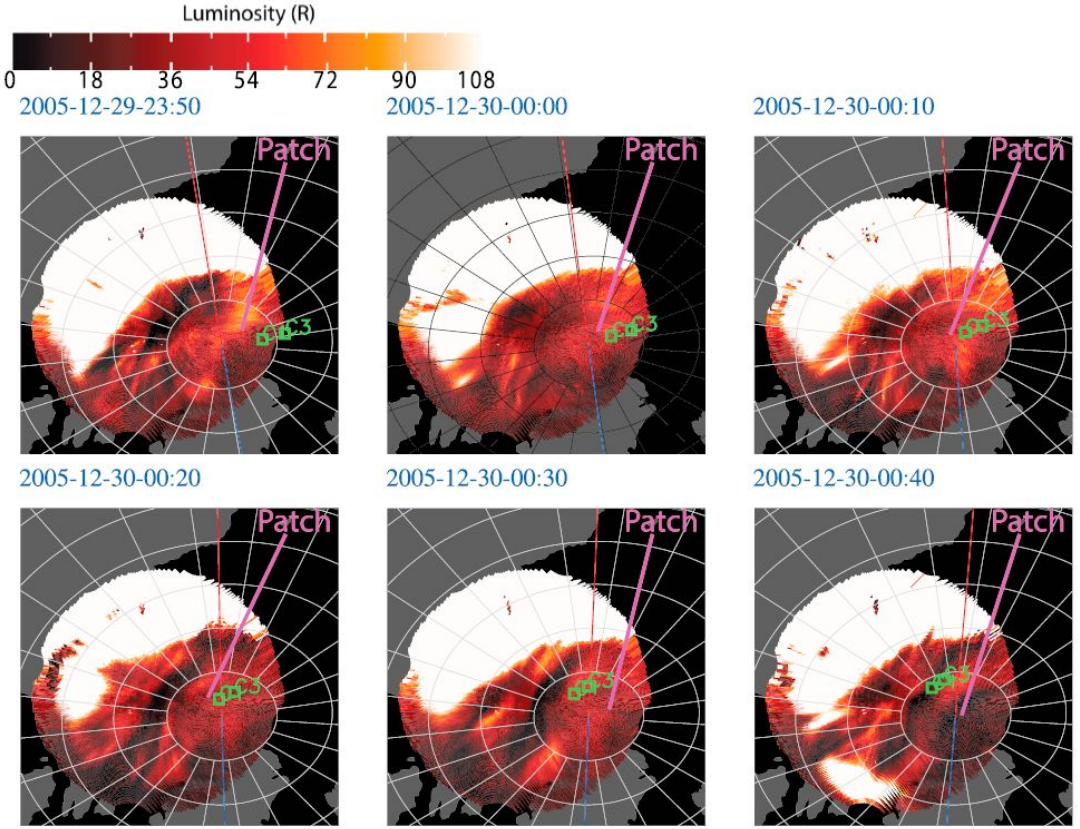
Luminosity (R)
0
18
36
54
72
90
108
2005-12-29-23:50
2005-12-30-00:00
2005-12-30-00:10
2005-12-30-00:20
2005-12-30-00:30
2005-12-30-00:40
Patch

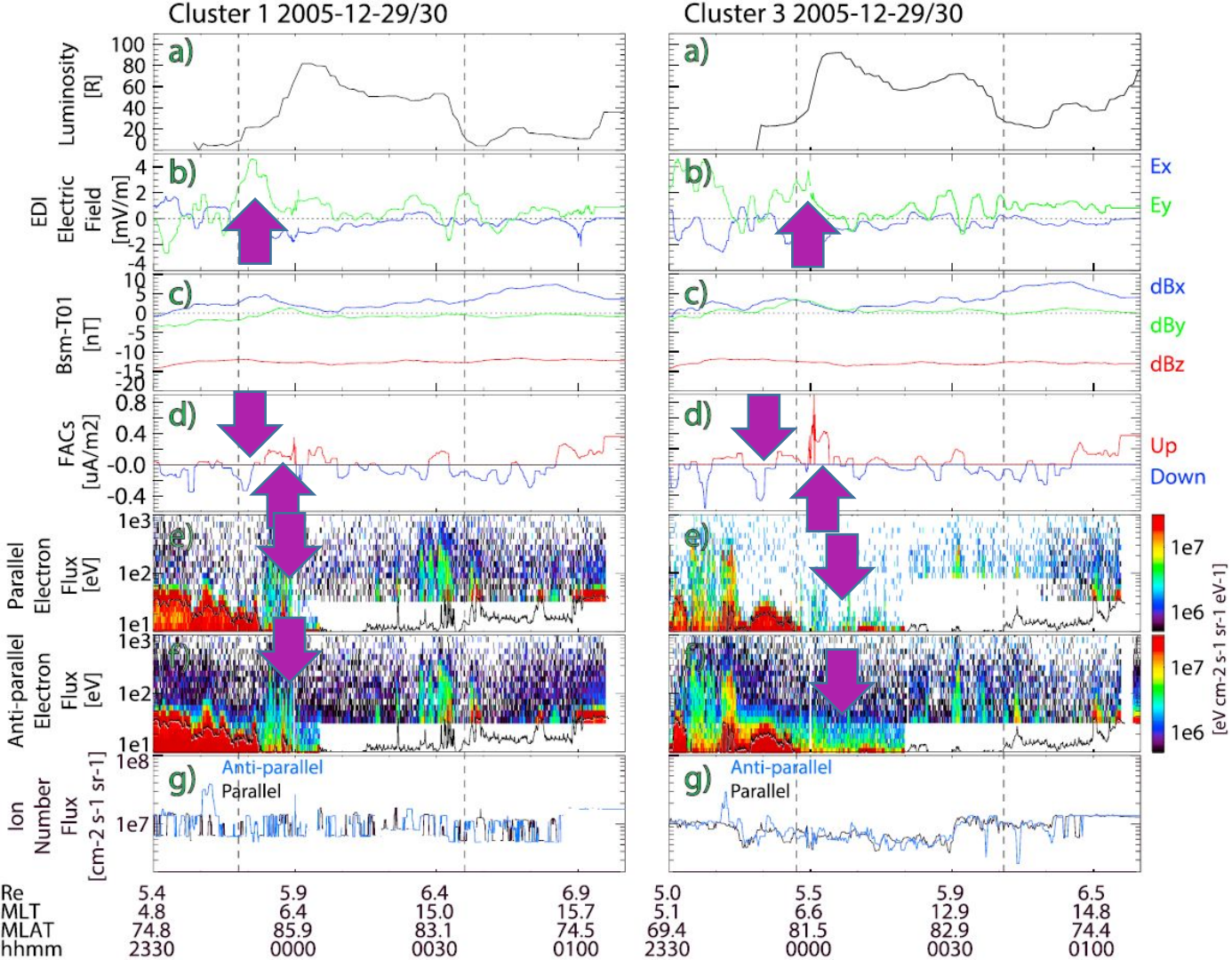
Cluster 1 2005-12-29/30
Cluster 3 2005-12-29/30
a)
Luminosity [R]
b)
EDI Electric Field [mV/m]
Ex
Ey
c)
Bsm-T01 [nT]
dBx
dBy
dBz
d)
FACs [uA/m2]
Up
Down
e)
Parallel Electron Flux [eV]
Anti-parallel Electron Flux [eV]
1e7
1e6
[eV cm-2 s-1 sr-1 eV-1]
g)
Ion Number Flux [cm-2 s-1 sr-1]
Anti-parallel
Parallel
Re 5.4 5.9 6.4 6.9 5.0 5.5 5.9 6.5
MLT 4.8 6.4 15.0 15.7 5.1 6.6 12.9 14.8
MLAT 74.8 85.9 83.1 74.5 69.4 81.5 82.9 74.4
hhmm 2330 0000 0030 0100 2330 0000 0030 0100

Stagnant enhancement

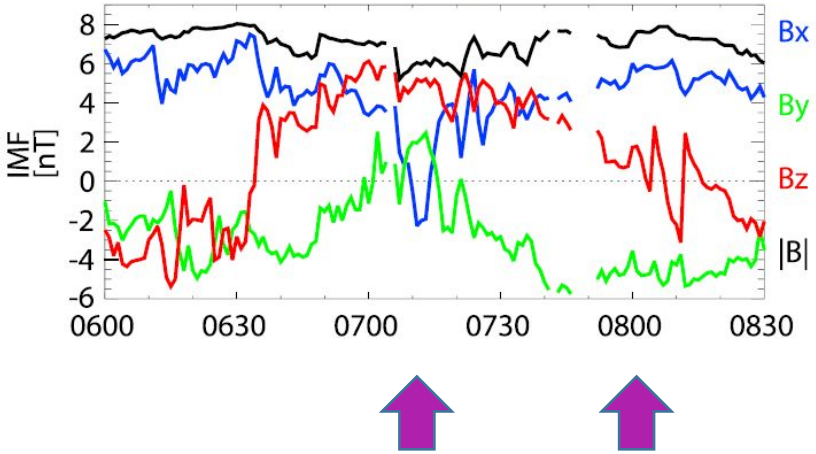

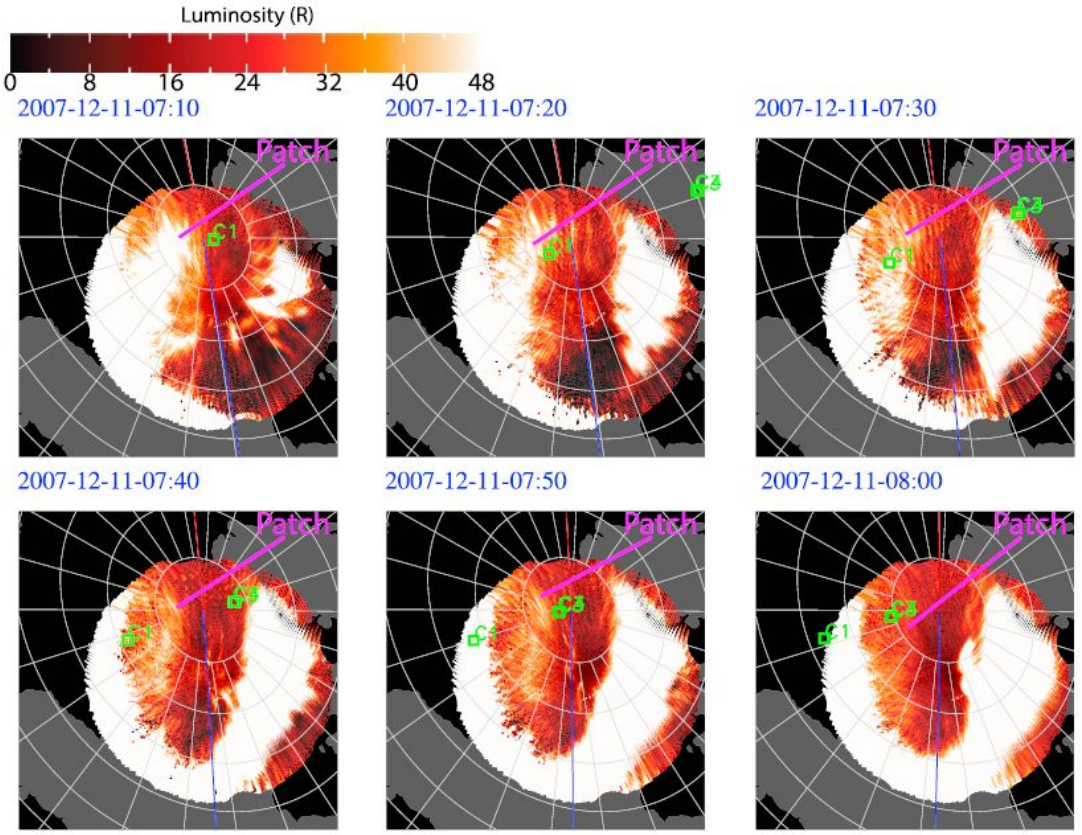

Stagnant enhancement

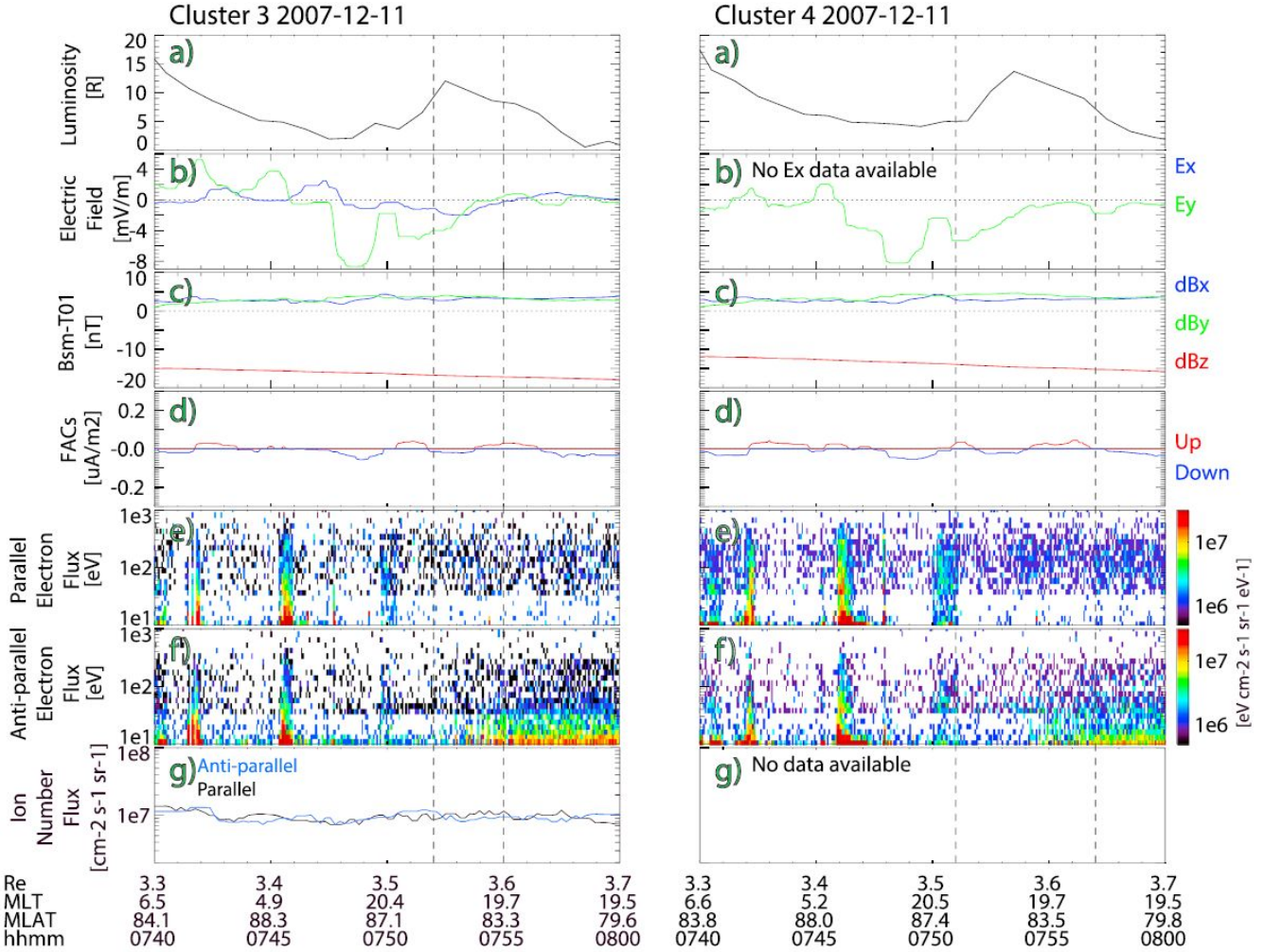

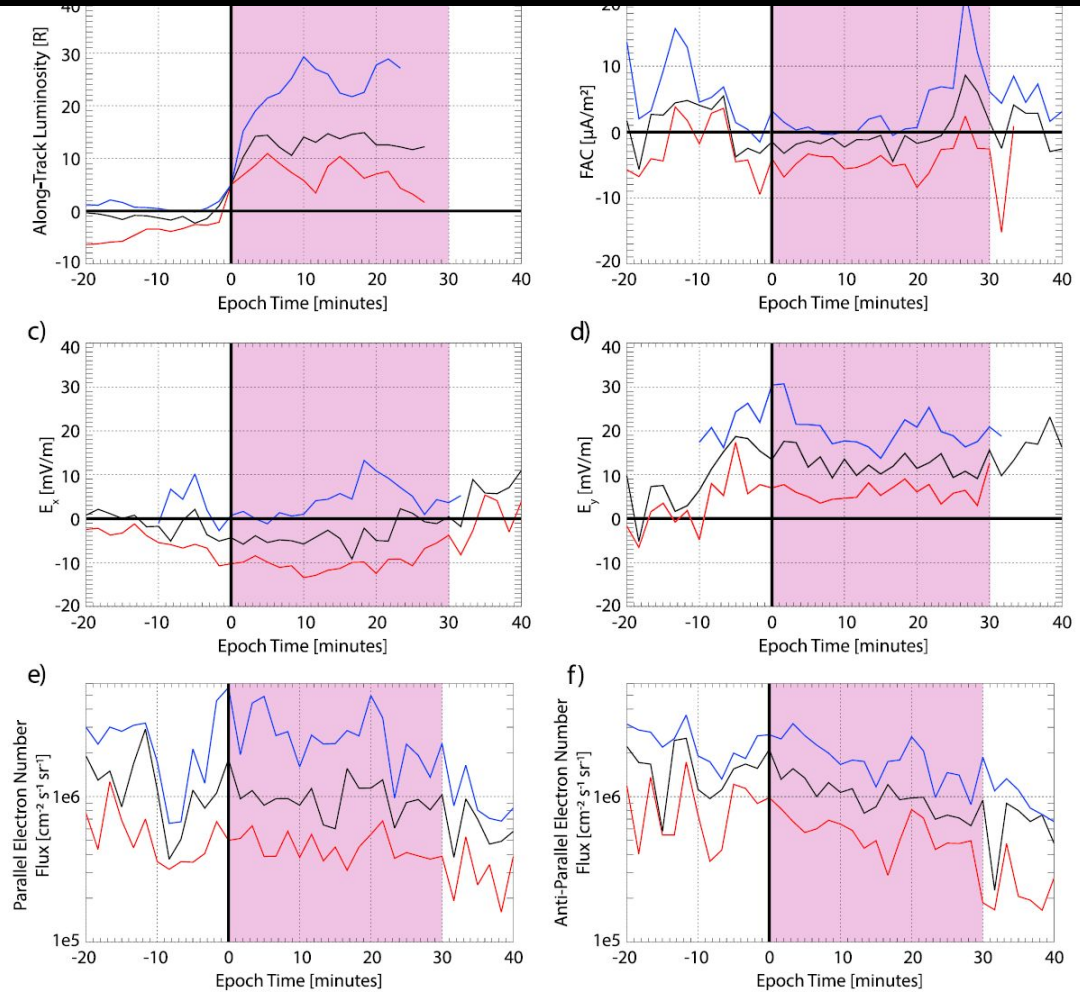

Figure 8. Superposed epoch studies performed with respect to the leading edge of each patch, where the red line is the 25 percentile, the black line is the median, and the blue line is the 75 percentile. The shaded purple region indicates the approximate patch width. (a) Along-track luminosity, where the leading edge is normalized to 5 R. (b) Field-aligned current at 250 km. (c) Ex at 250 km. (d) Ey at 250 km. (e) Parallel electron number flux at the Cluster spacecraft altitudes. (f) Antiparallel electron number flux at the Cluster spacecraft altitudes.

[3] Goodwin, L. V., Nishimura, Y., Coster, A. J., Zhang, S., Nishitani, N., Ruohoniemi, J. M., ... & Zhang, Q. H. (2020). Dayside Polar Cap Density Enhancements Formed During Substorms. *Journal of Geophysical Research: Space Physics*, *125*(10), e2020JA028101.

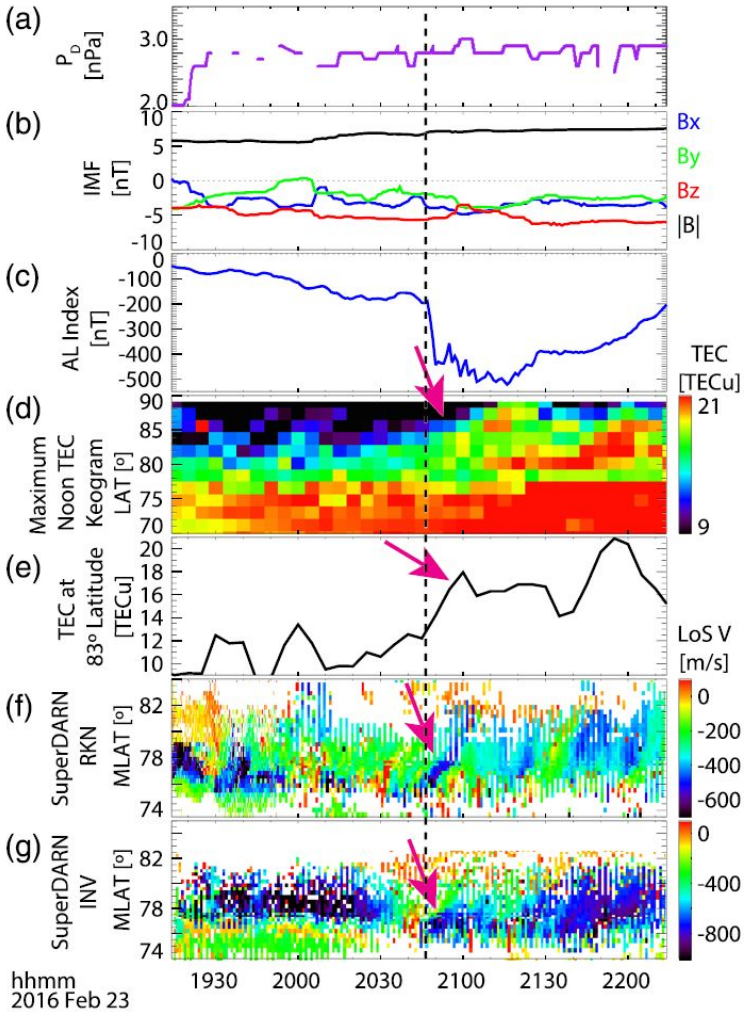

Figure 1. A polar cap patch formation event during a 23 February 2016 substorm beginning at 20:44UT. (a) Dynamic pressure. (b) IMF Bx, By, Bz, and |B|. (c) AL and AU indices. (d) TEC keogram around noon as a function of MLAT and UT. (e) TEC at 83◦ MLAT around noon. (f) Line-of-sight ion velocity data from the Rankin Inlet radar (Beam 5). (g) Line-of-sight ion velocity data from the Inuvik radar (Beam 13). The pink arrows indicate density enhancements in panels (d) and (e), as well as fast flows in panels (f) and (g). The substorm onset is indicated by a black dashed line.

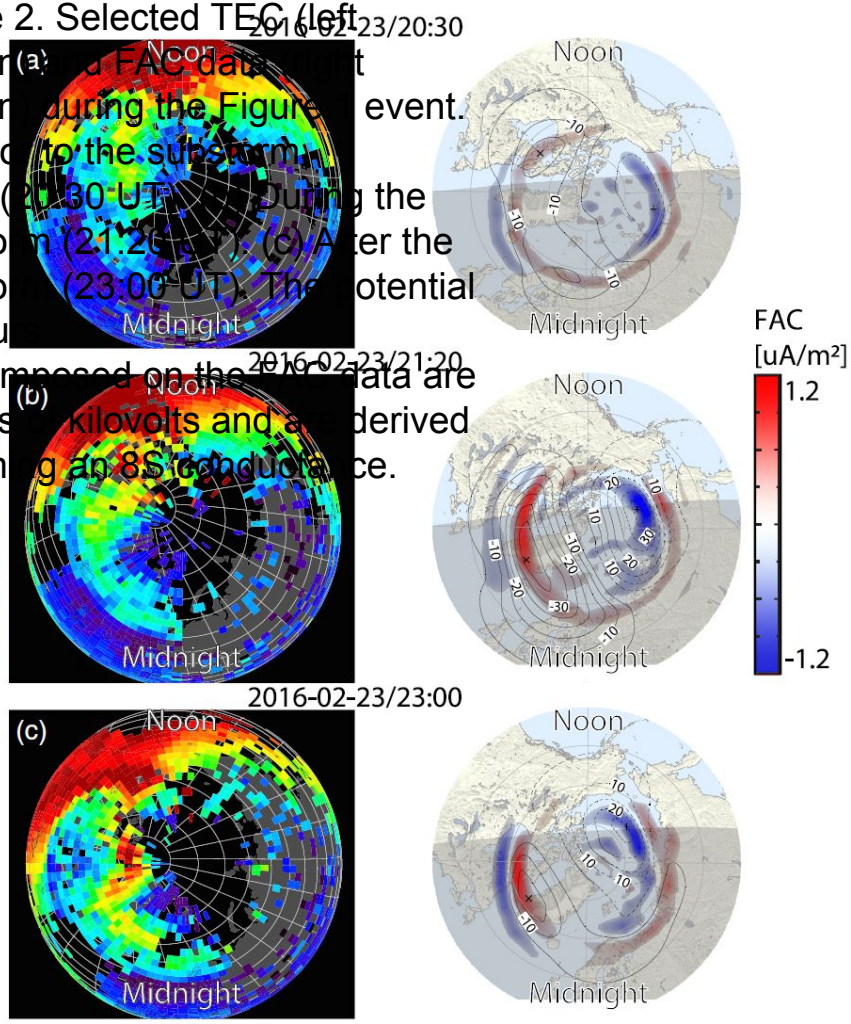

Figure 2. Selected TEC (left column) and FAC data (right column) during the Figure 1 event. (a) Prior to the substorm onset (20:30 UT). (b) During the substorm (21:20 UT). (c) After the substorm (23:00 UT). The potential contours superimposed on the FAC data are in units of kilovolts and are derived assuming an 8S conductance.

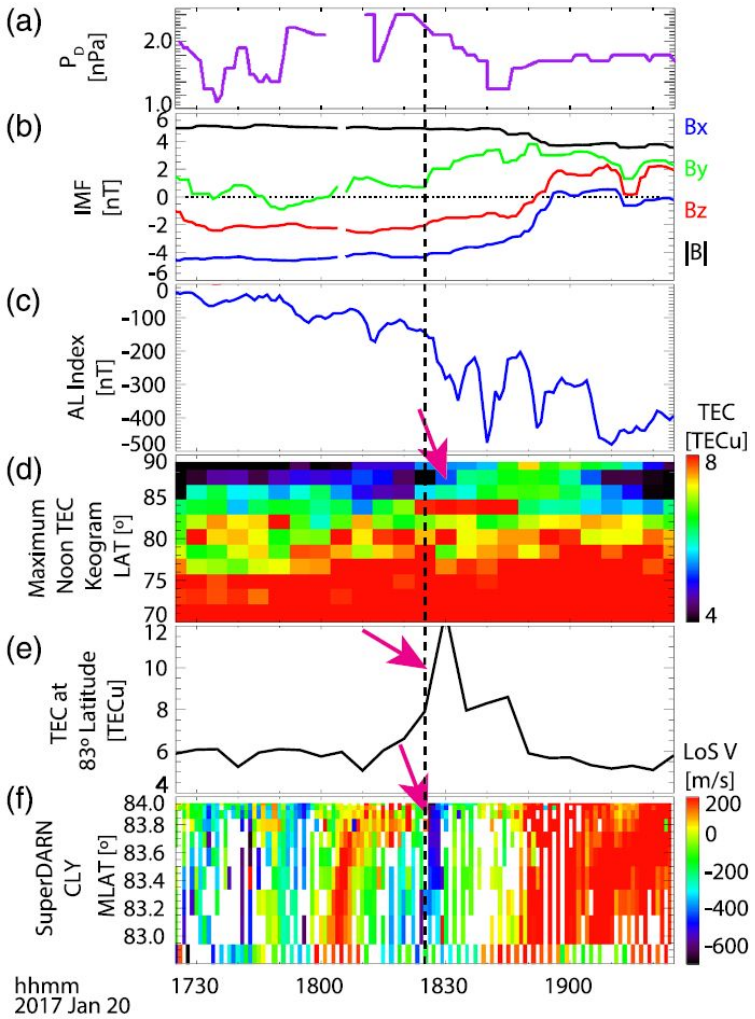

Figure 3. A polar cap patch formation event during a 20 January 2017 substorm beginning at 18:25UT. (a) Dynamic solar wind pressure. (b) IMF Bx, By, Bz, and |B|. (c) AL and AU indices. (d) TEC keogram around noon as a function of MLAT and UT. (e) TEC at 83◦ MLAT around noon. (f) Line-of-sight ion velocity data from the Clyde River radar (Beam 13). The pink arrows indicate TOIs and density enhancements in panels (d) and (e), and fast flows in panel (f). Substorm onset is indicated by a black dashed line.

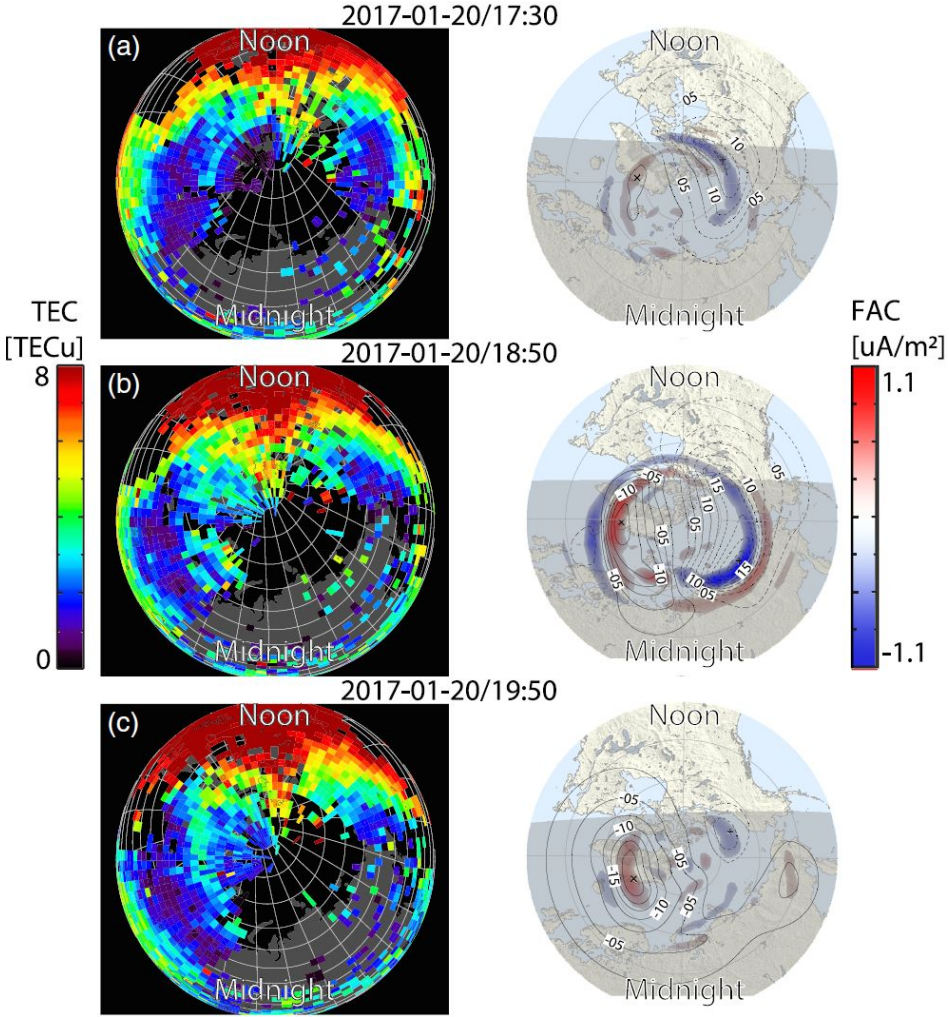

Figure 4. Selected TEC (left column) and FAC data (right column) during the Figure 3 event. (a) Prior to the substorm onset (17:30 UT). (b) During the substorm (18:50 UT). (c) Near the end of the substorm (19:50 UT). The potential contours superimposed on the FAC data are in units of kilovolts and are derived assuming an 8S conductance.

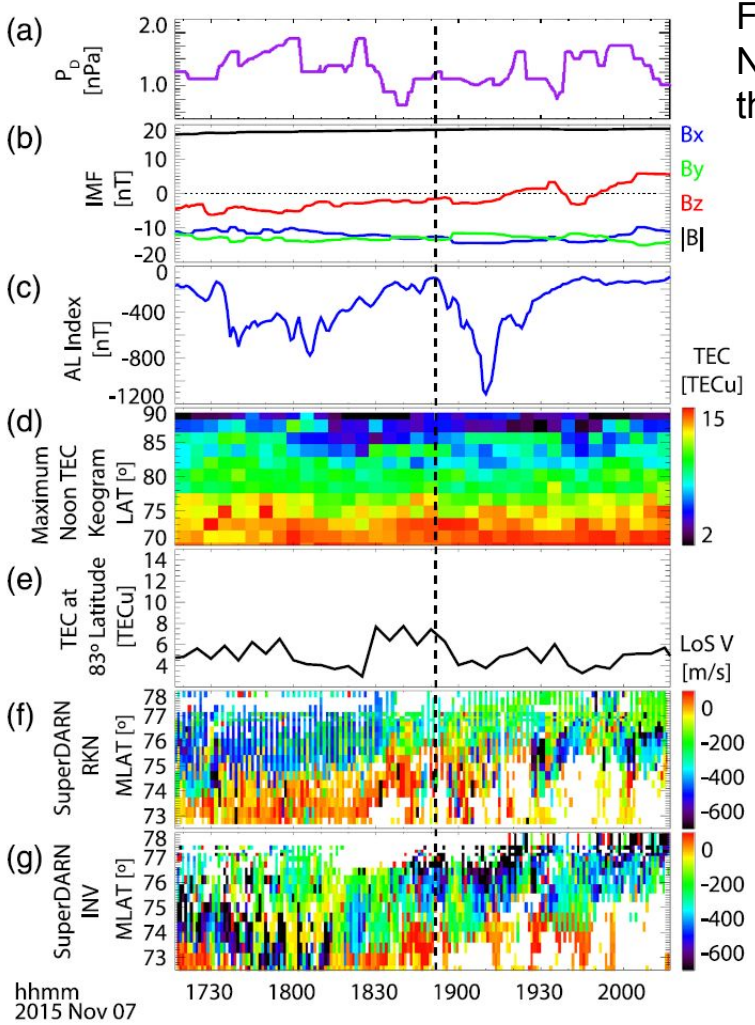

Figure 5. A polar cap patch formation event during a 7 November 2015 substorm beginning at 18:47 UT. Presented in the same format as Figure 1.

Figure 6. TEC data (left column, presented in the same format as Figure 2) and FAC data (right column) from 7 November 2015 [illegible] with superimposed equipotential maps. This data is presented in the same format as Figure 2.

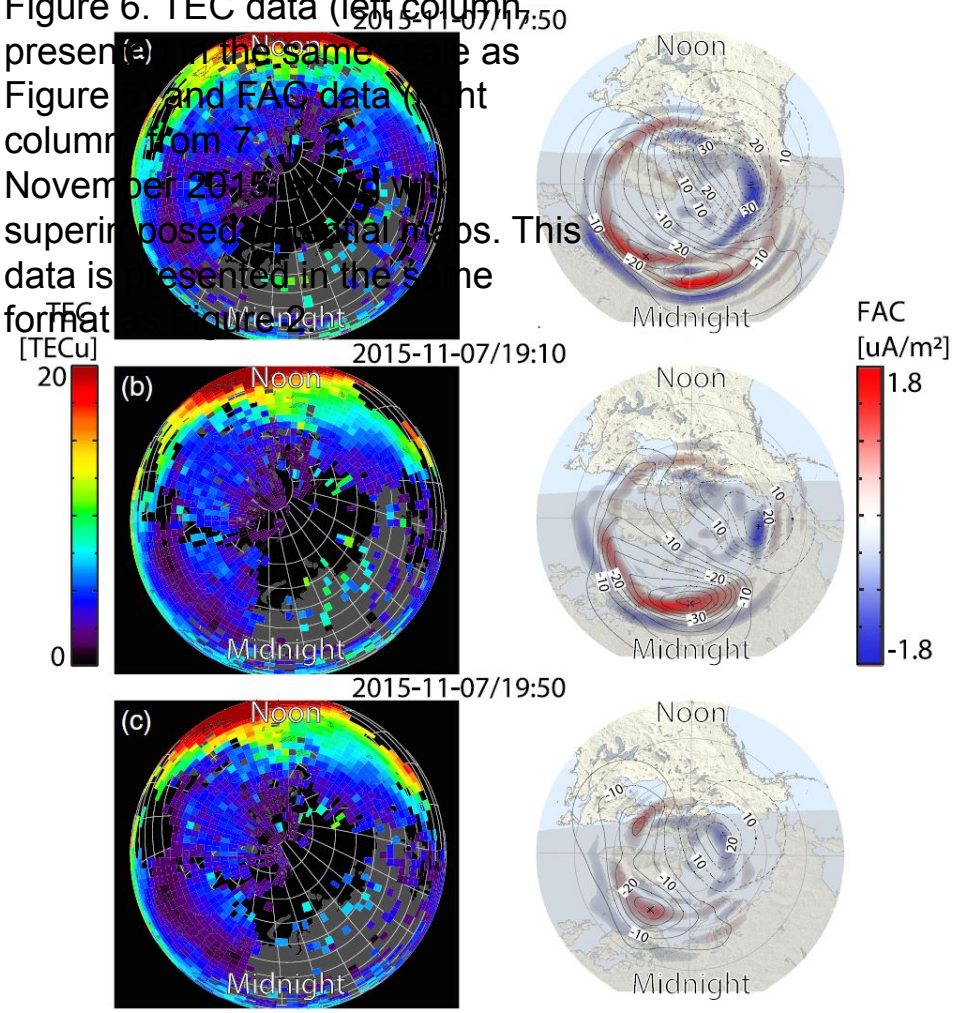

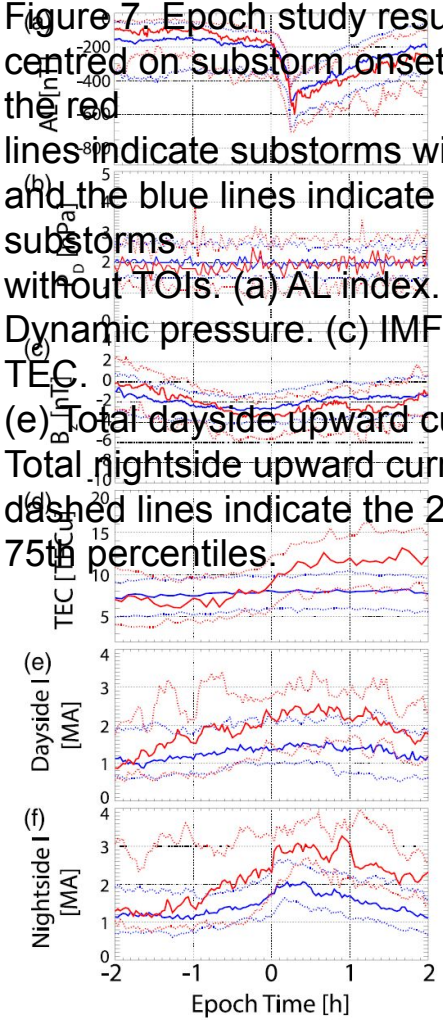

Figure 7. Epoch study results centred on substorm onset, where the red lines indicate substorms with TOIs and the blue lines indicate substorms without TOIs. (a) AL index. (b) Dynamic pressure. (c) IMF Bz. (d) TEC. (e) Total dayside upward current. (f) Total nightside upward current. The dashed lines indicate the 25th and 75th percentiles.

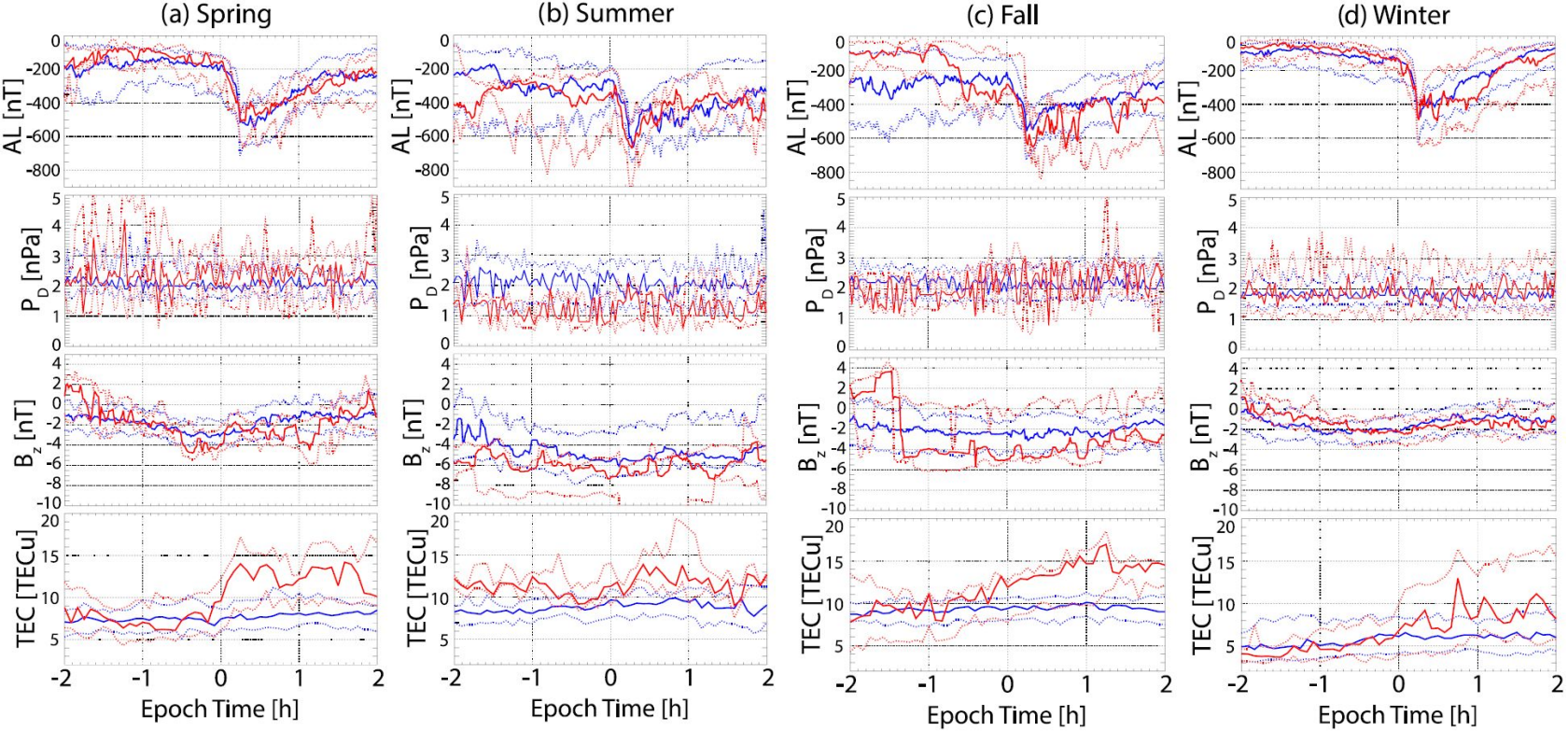
(a) Spring
(b) Summer
(c) Fall
(d) Winter
AL [nT]
P_D [nPa]
B_z [nT]
TEC [TECu]
Epoch Time [h]